IEEE Access
Multidisciplinary | Rapid Review | Open Access Journal

Received May 25, 2020, accepted June 13, 2020, date of publication June 19, 2020, date of current version July 1, 2020.

Digital Object Identifier 10.1109/ACCESS.2020.3003813

Throughput and Energy Efficiency of Cooperative ARQ Strategies for VANETs Based on Hybrid Vehicle Communication Mode

SUOPING LI[1,2], (Member, IEEE), FAN WANG[1], JAAFAR GABER[3], (Member, IEEE), AND XIAOKAI CHANG[2]

[1]School of Electrical and Information Engineering, Lanzhou University of Technology, Lanzhou 730000, China
[2]School of Science, Lanzhou University of Technology, Lanzhou 730000, China
[3]Department of Computer Science and Computer Engineering, Universite de Technologie Belfort-Montbeliard, 90010 Belfort, France

Corresponding author: Suoping Li (lsuop@163.com)

This work was supported in part by the National Natural Science Foundation of China under Grant 61663024, in part by the Erasmus+ Programme of European Commission under Grant 573879-EPP-1-2016-1-FR-EPPKA2-CBHE-JP, and in part by the Hongliu First Class Discipline Development Project of Lanzhou University of Technology, China.

ABSTRACT Vehicular ad-hoc networks (VANETs) are promising research areas which mainly include three communication modes: vehicle-to-vehicle (V2V), vehicle-to-infrastructure (V2I) and hybrid vehicle communication (HVC). But most of the current research on HVC mode in which vehicle nodes and infrastructures coexist only focuses on the analysis of the optimal single-type relay selection schemes. Inspired by this, in order to design an optimal multi-relay selection scheme which can select different types of relays simultaneously, and to compare it with single-type schemes, this paper firstly introduces a more practical network scenario by proposing a four-node system model which considers communication links between relays and building different channel models for different types of links. Four optimal relay selection protocols, which are named as Non-OR, SOR-AP, SOR-V and DOR-APV respectively, are then designed from the perspective of the different types and numbers of selected relays. The exact expressions of outage probability for each protocol are calculated based on the automatic repeat request (ARQ) protocol to evaluate the link interruption of the four protocols. Furthermore, this paper establishes a generalized 2-dimensional discrete time Markov chain (DTMC) model and analyzes the one-step state transition probability for each protocol. The closed-form expressions of system throughput and energy efficiency are derived by calculating the steady state distribution of the DTMC. Finally, the simulation results summarize the suitable network scenarios for which the four proposed protocols are recommended by comparing their system performance, so as to provide some suggestions for the future design and optimization of vehicle mobile networks.

INDEX TERMS VANETs, outage probability, relay selection, throughput, energy efficiency.

I. INTRODUCTION

Since the 21st century, the booming automobile industry and the popularity of private cars have made the road safety and traffic accidents become a global public safety problem. At the same time, with the rapid development of information and communication technology, how to provide safe and efficient communication services for drivers through the increasingly developed wireless network has become hotspot issues of both industrial and academic communities. In addition, passengers also demand more entertainment services during the trip, such as high-speed Internet access, video streaming services, multiplayer games and roadside advertising. Therefore, as one of the key components of the intelligent transportation system (ITS), vehicular ad-hoc networks (VANETs) emerge. VANETs were first proposed by International Telecommunication Union Telecommunication Standardization Sector (ITU-T) in 2003 [1], aiming to build a mobile communication platform for vehicles which not only improves traffic efficiency, but also provides more safety for drivers and more comfort for passengers.

The associate editor coordinating the review of this manuscript and approving it for publication was Faisal Tariq.

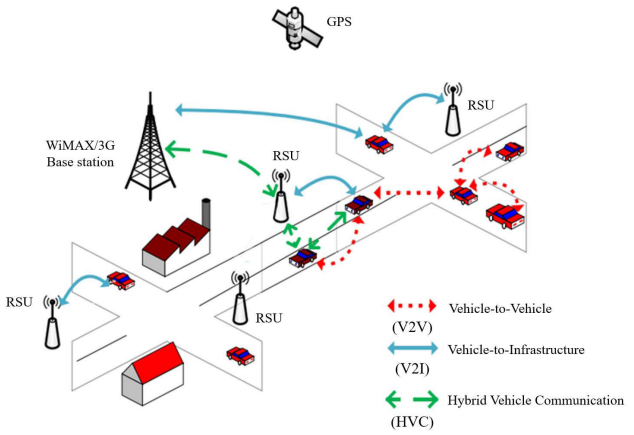

FIGURE 1. The structure of VANETs.

The structure of VANETs is shown in Figure 1, from which it can be clearly seen that there are mainly three communication modes in VANETs, i.e., vehicle-to-vehicle (V2V) (or inter-vehicle communication (IVC)), vehicle-to-infrastructure (V2I) (or roadside-vehicle communication (RVC)), and hybrid vehicle communication (HVC) which includes both V2V and V2I. In 2007, based on an extensive measurement campaign evaluating the performance of IEEE 802.11 in V2V and V2I, [2] not only verified the feasibility of VANETs in terms of extending the transmission range of infrastructures and connection time for mobile vehicles, but also drew an important conclusion that distance and line of sight (LoS) communication are the two main factors affecting the vehicular network communication. Therefore, it is crucial to design efficient transmission strategies to combat poor channel quality caused by fading factors (such as noise, path loss, multi-path effect, etc.), enhance communication reliability and reduce transmission error rate.

Cooperative communication, also known as virtual multiple input multiple output (MIMO), provides the receiver with extra diversity gain by introducing relays to help data transmission between the source and destination, has been proved to be an effective technology against path loss in [3]. On the other hand, automatic repeat request (ARQ) protocol is one of the most commonly used error control techniques. In wireless communication, signal fading and noise interference seriously affect the transmission condition and channel quality, repeated and low-quality retransmissions not only consume a lot of system energy, but also degrade the system performance. Therefore, a combined technology named as cooperative ARQ, which not only effectively provides diversity gain but also ensures the reliability of data transmission, has been proved to be an effective method to improve the transmission capacity of wireless mobile networks [4]–[6]. For example, a novel distributed cooperative ARQ scheme for IEEE 802.11 wireless networks has been proposed in our finished work [4] to evaluate the improvement in throughput and average packet transmission delay compared with its non-cooperative counterpart. The performance of ARQ over double Rayleigh channels which can be used to model the fading amplitude for V2V is studied in [5], analytical expressions of outage capacity, the average number of transmissions, and the average transmission rate are derived to demonstrate a conclusion that ARQ enables the transmitter to communicate at a rate close to the ergodic capacity even in absence of channel state information (CSI) at the transmitter, underscoring the importance of ARQ in improving the spectral efficiency and reliability of vehicular communication systems.

A. RELATED WORK

Until now, many related works on VAENTs have been proposed and they can be classified according to the three communication modes. Among them, the V2V mode [7]–[12] has always been the main object of research. To be specific, [7] investigates the end-to-end performance of multihop-V2V systems with regenerative and non-regenerative relays under n^*Rayleigh distribution, closed-form expressions for the outage probability with maximum ratio combining (MRC) diversity reception and the amount of fading are derived to prove a fact that the efficiency of regenerative and non-regenerative systems is closely related to the cascading order n. The outage probability of two-hop vehicular networks is analyzed in [8] and [9], the former mainly proposes three optimal relay selection criteria while the latter devotes to evaluate the impact of the power allocation on the outage probability, both of them derive the exact closed-form expressions for the outage probability and validate their results by Monte-Carlo simulation. Based on the optimal single relay selection criteria proposed in [8], some multiple best relays selection schemes [10]–[12] are designed. Reference [10] investigates the secrecy outage performance of dual-hop V2V system by designing two Kth best relay selection schemes, derives closed-form analytical expressions for secrecy outage probability of two proposed schemes and then verifies with Monte-Carlo simulations. References [11], [12] study the Nth best partial and opportunistic relay selection strategies under some objective questions such as hardware impairment and interference constraint. Besides [11] and [12]–[14] investigate the system performance of dual-hop decode-and-forward (DF) relaying vehicular networks in the presence of co-channel interference, where [13] examines the effect of relay geometry on system performance by calculating the upper bounds of outage probability and symbol error probability expressions for high signal-to-noise ratio (SNR), [14] maximizes the number of accessed communication links with the lowest power cost and satisfies the required quality of service (QoS) by proposing an innovative interference management method which considers link selection, power adaption, and communication mode selection simultaneously.

As for the research on V2I mode [15]–[19], the coverage and capacity requirements of the V2I link implemented by three systems which include digital broadcasting, cellular communication, and dedicated short-range communication (DSRC) are analyzed and compared in [15]. Focusing on the limited transmission range and capacity of VANETs,

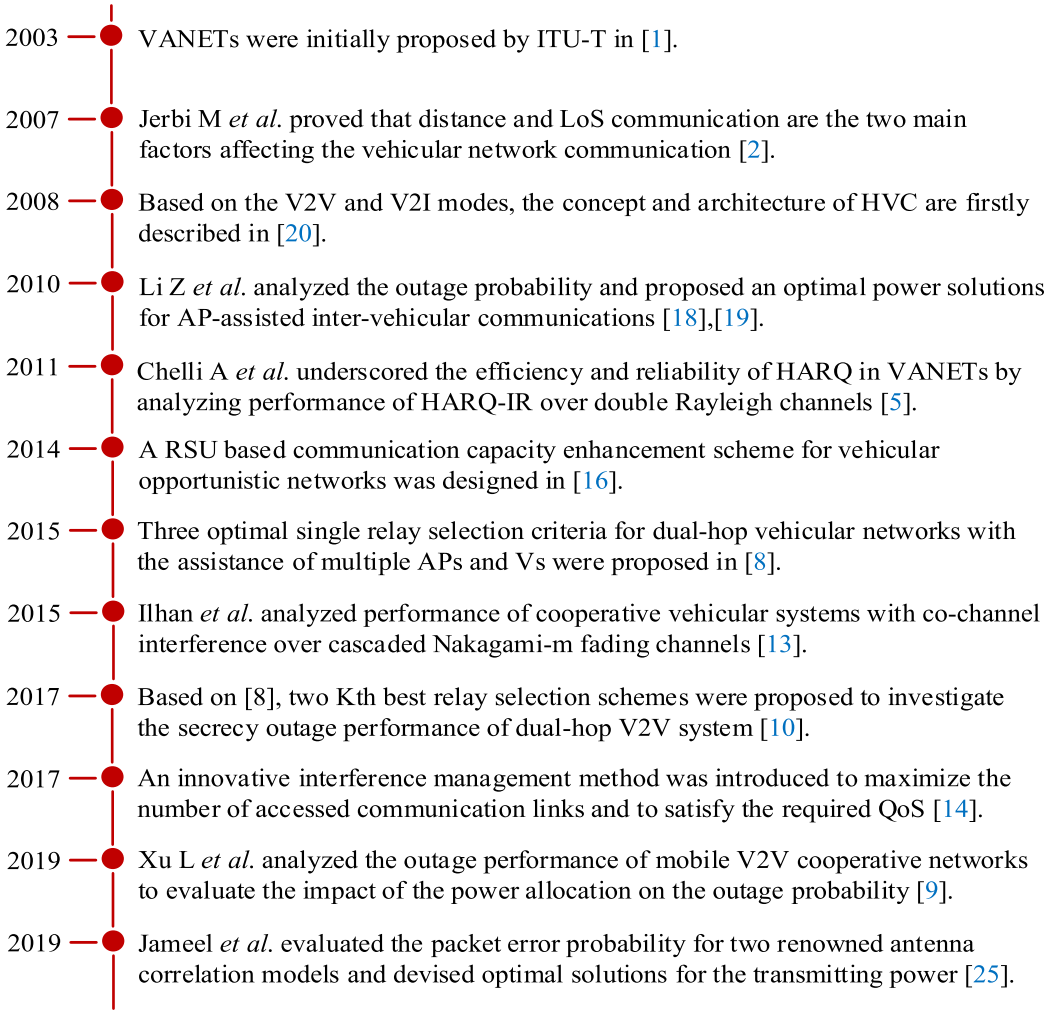

FIGURE 2. Timeline of VANETs.

some road side unit (RSU)-based communication capacity enhancement schemes are proposed in [16] and [17] to significantly improve the communication capability of V2I systems. Moreover, based on access point (AP)-assisted inter-vehicular communications, Li *et al.* [18], [19] derive the optimal power allocation (OPA) solutions by maximizing source-to-destination channel capacity assuming amplify-and-forward (AF) relaying, and then present the lower bound on outage probability at medium to high SNR.

Compared with V2V and V2I, there are only a few researches have concentrated on HVC mode [8], [20]–[28]. [20] initially described the architecture and benefits of the vehicle-to-vehicle-to-infrastructure (V2V2I), i.e., HVC mode, in 2008. Performance such as outage probability and symbol error rate (SER) of VANETs with the assistance of multiple APs and vehicles (Vs) is analyzed in [21]–[24]. Furthermore, under a more practical uplink scenario where antennas at the RSU experience correlated fading, Jameel *et al.* [25] evaluate the packet error probability for two renowned antenna correlation models and devise optimal solutions for the transmitting power. Recently, in order to simultaneously overcome spectrum scarcity and network connectivity issues, an idea of introducing the cognitive radio (CR) technology into VANETs, i.e., CR-VANETs, has become popular [26]–[28]. Based on the dense and sparse network conditions which respectively represent city and highway scenarios, [26] proposes an infrastructure-aided hybrid routing protocol that uses a RSU to help vehicular nodes to select idle channels and relays. The optimal relay is selected by calculating the minimum message delivery time among all the neighboring nodes. Simulation results prove a better performance in delay, delivery ratio and overhead compared with other two existing techniques. An optimization protocol which coordinates the enhanced optimal link state routing protocol (MMPR-OLSR) with the GSA-PSO (gravitational search-particle swarm optimization) scheme is designed in [27] to select the suitable relays and to reduce the unnecessary overheads due to the propagation. The proposed method is simulated on the NS-2 platform.

Summarily, the development of VANETs and some representative state-of-the-art works are presented in Figure 2.

However, there are some shortcomings in the current researches of VANETs. Firstly, as mentioned above, the majority of research is focused on V2V and V2I, with just a few on HVC mode. Even though [8], [21]–[24], [26]–[28] are proposed for this purpose, the vehicle source is assisted only by multiple APs or Vs in these works. For example, Vehicle nodes in CR-VANETs can only select other vehicles as relays with the assistance of the RSU [26]. In other words, the source is only helped by single-type relays. To the best of our knowledge, there is no research on the performance analysis of VANETs with the assistance of both APs and Vs. Secondly, Much of the work almost selects Rayleigh, Nakagami-m or Rice, which is suitable for V2I mode, as the channel model of VANETs, but double (cascaded) Rayleigh or Nakagami-m fading channel can describe the V2V mode with two mobile terminals more accurately [5], [8], [29]. It is necessary to model different channels for different data links in the HVC mode. Finally, almost all of the above researches have obtained closed-form expressions of outage probability, but few of them evaluate some specific system performance, such as throughput, delay and energy efficiency, further. The accurate analysis of specific system performance can more intuitively evaluate and compare the pros and cons of the proposed scheme.

B. CONTRIBUTIONS AND PAPER STRUCTURE

Against the above background, our main contributions are summarized as follows:

a) The design of four optimal relay selection protocols. According to a fact that the vehicle source can be assisted by both APs and Vs in the HVC mode, from the perspective of selecting different types and numbers of relays, this paper proposes four optimal relay selection protocols based on a more practical network scenario. This scenario not only considers the data links between relays, but also adopts different channel models to describe the fading characteristics of links V2V and V2I, respectively.

b) The establishment of a novel discrete time Markov chain (DTMC) model. A generalized 2-dimensional DTMC model for the four proposed protocols is built and the one-step state transition probability for each protocol is separately analyzed to evaluate the system performance.

c) The derivation of closed-form expressions of system performance. Based on the outage probability analysis, this paper obtains the closed-form expressions of system throughput and energy efficiency under arbitrary maximum transmission number for the four proposed protocols by calculating the steady state distribution of the DTMC.

d) The numerical simulations with MATLAB verify the influence of network parameters such as the maximum transmission number and the location of relays on system performance, and compare the performance of the four proposed protocols.

The rest of this paper is organized as follows: the system model and channel model of VANETs with HVC are introduced in Section II. Section III proposes four optimal relay selection protocols and analyzes the outage probability of each protocol. A generalized 2-dimensional DTMC is established to obtain the one-step state transition probability for the four proposed protocols in Section IV. System performance analysis including throughput and energy efficiency and MATLAB numerical simulations are shown in Section V and Section VI, respectively. Finally, the conclusion and expectation are presented in Section VII.

II. MODEL OF VANETS BASED ON HVC MODE

In this section, we will build both system and channel models for VANETs with HVC mode. Furthermore, the main assumptions used are described.

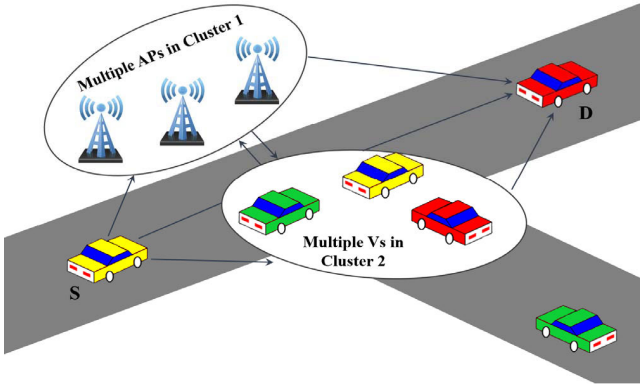

FIGURE 3. A VANET with the assistance of multiple APs and Vs.

A. SYSTEM MODEL

As shown in Figure 3, this paper considers a VANET consisting of a vehicle source node (S), a vehicle destination node (D), and multiple APs and Vs. For convenience, multiple APs and Vs are assumed to be located in clusters 1 and 2, respectively. Each node in the VANET is equipped with a single antenna and operates in the half-duplex mode, i.e., nodes cannot send and receive information simultaneously in the same bandwidth.

It is clear from Figure 3 that the VANET based on HVC can be equivalent to a four-node system model shown in Figure 4, i.e., there are two optimal candidate relays (AP and V) in the VANET assist in the communication between a pair of S and D. It is worth noting that the two optimal candidates AP and V are the best nodes with the highest instantaneous SNR selected from cluster 1 and cluster 2, respectively. Both AP and V work in the DF mode. It is also assumed that the corresponding receiver can well know CSI and all nodes keep perfect synchronization between each other.

The symbol $h_{i,j}$ in Figure 4 represents the channel fading gain of link i-j, where $i \in (S, AP, V)$, $j \in (AP, V, D)$ and $i \neq j$. It is worth noting that two additional links between relays (i.e., links AP-V and V-AP) are creatively considered in this paper to make our analysis more consistent

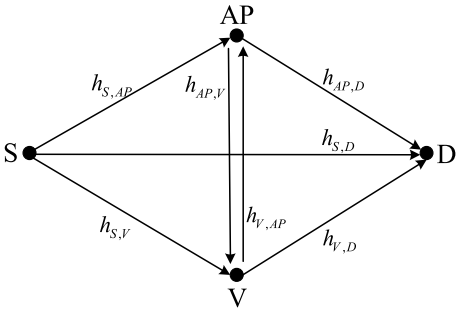

FIGURE 4. A four-node system model for VANET with HVC.

with the realistic broadcast nature of wireless channels than those works ignoring these links. Moreover, we assume that $h_{AP,V} = h_{V,AP}$ because of the same relative communication distance between AP and V.

B. CHANNEL MODEL

Because of the HVC, there are two different kinds of communication links (i.e., V2V links and V2I links) in the VANET and different channel models need to be built to describe and distinguish their different transmission characteristic. It is worth noting that the network environment considered in this paper is a crowded city scenario in which vehicle nodes are dense and always limited in speed. Compared with the sparse highway scenarios, the channel quality changes slowly in this environment, and the signal fading is mainly caused by path loss and shadow effect. Therefore, this paper adopts the slow fading channel model to approximate it.

To be specific, a flat Rayleigh slow fading channel is adopted as the channel model of V2I links (i.e., links S-AP, AP-D, and AP-V(V-AP)) where only one node has mobility. Obviously, the channel fading gain $h_{i,j}$ of V2I link *i-j* is a complex Gaussian random variable (RV) with zero mean and $\sigma_{i,j}^2$ variance, i.e., $h_{S,AP} \sim CN\left(0, \sigma_{S,AP}^2\right)$, $h_{AP,D} \sim CN\left(0, \sigma_{AP,D}^2\right)$ and $h_{AP,V} \sim CN\left(0, \sigma_{AP,V}^2\right)$. As for the V2V links (links S-D, S-V and V-D), according to the measurement results shown in [30] that if vehicles are driving in the middle lanes of highways or in an urban environment, then the double-bounce scattering components caused by fixed scatterers are dominant. Therefore, the double-bounce scattering mechanism has been assumed in several V2V channel models, such as the two-ring model [31], the street model [32], and the T-junction street model [33]. Under double-bounce scattering conditions, the fading amplitude can be modeled as a double Rayleigh process [29], which can be expressed as a product of two independent Rayleigh processes. Therefore, the channel model of V2V links in this paper is assumed to be a flat double Rayleigh slow fading channel. In other words, $h_{S,D}, h_{S,V}$ and $h_{V,D}$ can be correspondingly expressed as the product of two independent and identically distributed (i.i.d) complex Gaussian RVs, i.e., $h_{S,D} \triangleq h_{S,D,1} \cdot h_{S,D,2}$, $h_{S,V} \triangleq h_{S,V,1} \cdot h_{S,V,2}$ and $h_{V,D} \triangleq h_{V,D,1} \cdot h_{V,D,2}$, where RVs: $h_{S,D,1}(h_{S,D,2})$, $h_{S,V,1}(h_{S,V,2})$ and $h_{V,D,1}(h_{V,D,2})$ are complex Gaussian RVs with zero mean and variances: $\sigma_{S,D,1}^2(\sigma_{S,D,2}^2)$, $\sigma_{S,V,1}^2(\sigma_{S,V,2}^2)$ and $\sigma_{V,D,1}^2(\sigma_{V,D,2}^2)$, respectively. The noise model used in this paper is an additive white Gaussian noise (AWGN) with zero mean and δ^2 variance.

III. FOUR OPTIMAL RELAY SELECTION PROTOCOLS AND OUTAGE PROBABILITY ANALYSIS

The existence of two different types of relays in VANETs based on HVC provides a variety of alternative optimal relay selection schemes. In general, there are mainly three schemes according to the different number of selected relays which is denoted as $N, N \in (0, 1, 2)$. That is, schemes not choosing any relay ($N = 0$), choosing a single optimal relay ($N = 1$), and choosing two optimal relays ($N = 2$). Furthermore, in terms of the scheme choosing single relay, two schemes for selecting different types of relays (i.e., choosing either AP or V) are extended according to the mobility of relays. Which is the best one? Inspired by the above ideas, this paper proposes four different selection protocols and analyzes their system performance. To be specific, they are Non-OR (Non-Optimal Relay) protocol, SOR-AP (Single Optimal Relay-Access Point) protocol, SOR-V (Single Optimal Relay-Vehicle) protocol and DOR-APV (Dual Optimal Relays- Access Point and Vehicle) protocol, respectively.

This paper refers to the duration for sending a certain data frame as an ARQ process, each transmission in which is called as an ARQ round, and the maximum transmission number in one ARQ process is set to L, which includes one direct transmission and L-1 retransmissions. For the four selection protocols, in the first ARQ round (i.e., the direct transmission from S), S transmits a data frame to AP, V and D. Since both AP and V work in DF mode, after the first ARQ round, AP, V and D incorrectly decode the data frame received from S with the outage probability of their corresponding links. In order to analyze the outage probability of different links, this paper denotes $F_X(x)$ as the cumulative distribution function (CDF) of RV X and $\omega_{ij} \triangleq \left|h_{i,j}\right|^2$. According to the conclusion drawn in [34]: the sum of squares of moduluses of joint Gaussian complex RVs with zero mean have exponential distribution. It can be deduced from section II that ω_{ij} of V2I link *i-j* is exponential distribution with parameter λ_{ij}. Based on [35], $\lambda_{ij} \propto d_{ij}^{\beta}$, where d_{ij} is the distance between node i and j, β is the path loss factor. In other words, ω_{SAP}, ω_{APD} and $\omega_{APV}(\omega_{VAP})$ are exponential distributions with parameters λ_{SAP}, λ_{APD} and $\lambda_{APV}(\lambda_{VAP})$, respectively, i.e. $\omega_{SAP} \sim e(\lambda_{SAP})$, $\omega_{APD} \sim e(\lambda_{APD})$ and $\omega_{APV}(\omega_{VAP}) \sim e(\lambda_{APV})$. Therefore, their CDFs can be directly calculated by $F_X(x) = 1 - e^{-\lambda_X x}(x > 0)$. As for RVs of V2V links: ω_{SD}, ω_{SV} and ω_{VD}, taking ω_{SD} as an example, its CDF $F_{\omega_{SD}}(v)$ can be obtained as follows:

$$\begin{aligned} F_{\omega_{SD}}(v) &= \Pr\{\omega_{SD} < v\} = \Pr\left\{\omega_{SD,1} \cdot \omega_{SD,2} < v\right\} \\ &= \Pr\left\{\omega_{SD,1} < \frac{v}{\omega_{SD,2}}\right\} \\ &= \int_0^{\infty} f_{\omega_{SD,2}}(x_2) \int_0^{\frac{v}{x_2}} f_{\omega_{SD,1}}(x_1) dx_1 dx_2 \end{aligned} \quad (1)$$

TABLE 1. Channel models and distribution characteristics of links in the VANET.

Link	Channel model	$h_{i,j}$	ω_{ij}	$F_{\omega_{ij}}(x)$
S-D	double Rayleigh	$h_{S,D,1}\cdot h_{S,D,2}$	$\lvert h_{S,D,1}\cdot h_{S,D,2}\rvert^2$	$1\text{-}2\lambda_{SD}\sqrt{x}K_1\left(2\lambda_{SD}\sqrt{x}\right)$
S-AP	Rayleigh	$h_{S,AP}$	$\lvert h_{S,AP}\rvert^2$	$1-e^{-\lambda_{SAP}x}$
AP-D	Rayleigh	$h_{AP,D}$	$\lvert h_{AP,D}\rvert^2$	$1-e^{-\lambda_{APD}x}$
S-V	double Rayleigh	$h_{S,V,1}\cdot h_{S,V,2}$	$\lvert h_{S,V,1}\cdot h_{S,V,2}\rvert^2$	$1\text{-}2\lambda_{SV}\sqrt{x}K_1\left(2\lambda_{SV}\sqrt{x}\right)$
V-D	double Rayleigh	$h_{V,D,1}\cdot h_{V,D,2}$	$\lvert h_{V,D,1}\cdot h_{V,D,2}\rvert^2$	$1\text{-}2\lambda_{VD}\sqrt{x}K_1\left(2\lambda_{VD}\sqrt{x}\right)$
AP-V (V-AP)	Rayleigh	$h_{AP,V}$	$\lvert h_{AP,V}\rvert^2$	$1-e^{-\lambda_{APV}x}$

formula (1) can be rewritten as (2) by using $f_{\omega_{SD,1}}(x_1) = \lambda_{SD}e^{-\lambda_{SD}x_1}$ and $f_{\omega_{SD,2}}(x_2) = \lambda_{SD}e^{-\lambda_{SD}x_2}$:

$$\begin{aligned} F_{\omega_{SD}}(v) &= \int_0^{\infty}\lambda_{SD}e^{-\lambda_{SD}x_2}\int_0^{\frac{v}{x_2}}\lambda_{SD}e^{-\lambda_{SD}x_1}dx_1dx_2 \\ &= \int_0^{\infty}\lambda_{SD}e^{-\lambda_{SD}x_2}\left(1-e^{-\lambda_{SD}\frac{v}{x_2}}\right)dx_2 \\ &= 1-\lambda_{SD}\int_0^{\infty}e^{-\lambda_{SD}x_2-\frac{\lambda_{SD}v}{x_2}}dx_2 \end{aligned} \tag{2}$$

according to $\int_0^{\infty}e^{-\frac{a}{4x}-bx}dx = \sqrt{\frac{a}{b}}K_1\left(\sqrt{ab}\right)$ from [36], $F_{\omega_{SD}}(v)$ can be finally expressed as:

$$F_{\omega_{SD}}(v) = 1\text{-}2\lambda_{SD}\sqrt{v}K_1\left(2\lambda_{SD}\sqrt{v}\right) \tag{3}$$

where $K_1(\cdot)$ is the second kind of modified Bessel function. Similarly, the CDFs of ω_{SV} and ω_{VD} can be obtained by replacing λ_{SD} in formula (3) with λ_{SV} and λ_{VD}, respectively. To sum up, the channel characteristics of all links in the VANET are summarized in Table 1. They will be used in the following outage probability analysis of four selection protocols.

A. NON-OR PROTOCOL

In the Non-OR protocol, i.e., $N = 0$, if D fails to decode the data frame correctly in an ARQ round, it requests a retransmission from S along the same transmission path by feeding back a NACK in this ARQ round. S does not stop retransmission until it receives an ACK from D or the maximum transmission number L is reached. Obviously, in this protocol, only the outage probability of link S-D needs to be discussed because no transmission behavior of relays is involved in.

This paper adopts ARQ protocol in which the receiver discards the data frame and requests retransmission once it cannot decode the data frame correctly, and the sender retransmits the data frame when it receives NACK from the receiver. We assume that the transmitting power at the sender $i, i \in (S, AP, V)$ is equal and denoted as P_t. Given the bandwidth $B = 1$, the maximum signaling rate (i.e., channel capacity) that the link X-Y can reach in an ARQ round is:

$$C_{XY} = \log_2(1+SNR_{XY}) = \log_2(1+\gamma\omega_{XY}) \tag{4}$$

where $SNR_{XY} = \frac{P_t\lvert h_{X,Y}\rvert^2}{N_0} = \gamma\omega_{XY}$, N_0 is the power spectrum density of AWGN and $\gamma P_t/N_0$. According to the Shannon information theory, the probability that the channel capacity is less than the signaling rate threshold r bits/slot/Hz is the outage probability. Then the joint outage probability $\Pr\left(XY_{out,l}\right)$ of link X-Y in the lth ARQ round can be expressed as:

$$\begin{aligned} \Pr\left(XY_{out,l}\right) &= \Pr\left\{C_{XY,1}<r\right\}\cdot\Pr\left\{C_{XY,2}<r|C_{XY,1}<r\right\} \\ &\quad\cdots\Pr\left\{C_{XY,l}<r|C_{XY,l-1}<r\right\} \\ &= \Pr\left\{C_{XY,1}<r,\cdots,C_{XY,l}<r\right\} \end{aligned} \tag{5}$$

Based on formula (5), $a_1 \triangleq (2^r-1)/\gamma$, the joint outage probability $\Pr\left(SD_{out,l}\right)$ in the lth ARQ round of Non-OR protocol can be obtained as follows:

$$\begin{aligned} \Pr\left(SD_{out,l}\right) &= \Pr^l\left\{\log_2(1+\gamma\omega_{SD})<r\right\} \\ &= \Pr^l\left\{\omega_{SD}<a_1\right\} = F^l_{\omega_{SD}}(a_1) \end{aligned} \tag{6}$$

B. SOR-AP(V) PROTOCOL

Based on the same selection principle, i.e., $N = 1$, the difference between protocols SOR-AP and SOR-V is that the former chooses AP but the latter chooses V as the optimal single relay to assist the failed transmission between S and D. For brevity, we denote $\tilde{R}, \tilde{R} \in (AP, V)$ as the optimal relay selected from SOR-AP(V) protocols. To be specific, S transmits a new frame in the next ARQ round if D decodes the data frame correctly in the current ARQ round. Otherwise, a NACK is fed back by D to request a retransmission. In the SOR-AP(V) protocols, if $\tilde{R}$ has successfully decoded the data frame before D, it performs the retransmission to D in subsequent ARQ rounds after receiving the NACK from D. Otherwise, the error frame is still retransmitted by S. In SOR-AP(V) protocols, S does not stop retransmission until it receives an ACK from D, or L is reached, or $\tilde{R}$ decodes the frame correctly and retransmits it. Obviously, besides $\Pr\left(SD_{out,l}\right)$, the joint outage probability of links S-$\tilde{R}$ and S-$\tilde{R}$-D (link S-D with cooperation of $\tilde{R}$) in the lth ARQ round, i.e., $\Pr\left(S\tilde{R}_{out,l}\right)$ and $\Pr\left(S\tilde{R}D_{out,l}\right)$, needs to be considered because the transmission behavior of $\tilde{R}$ is involved.

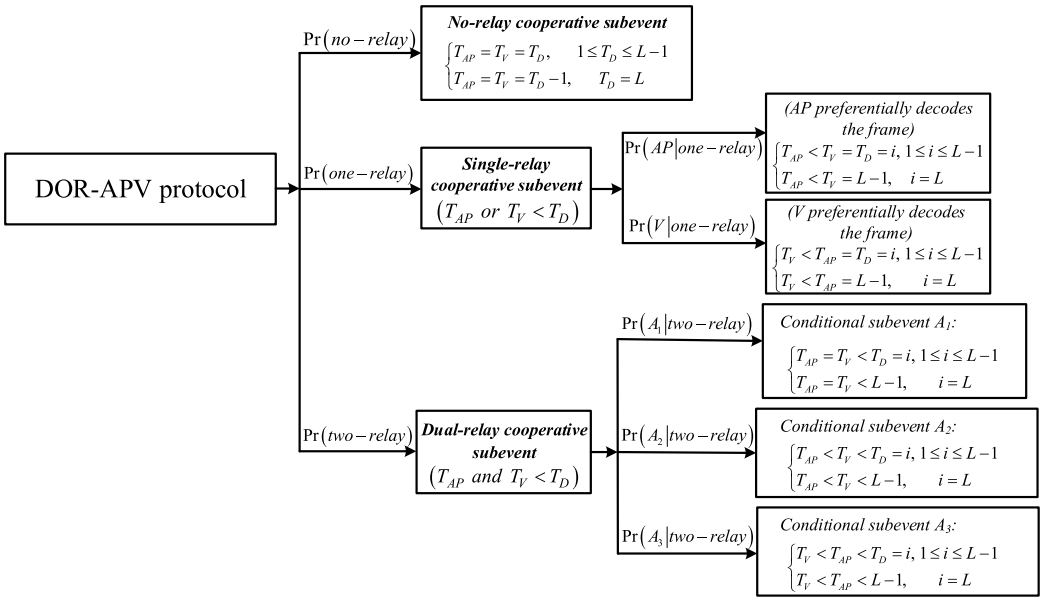

FIGURE 5. Cooperative subevents and corresponding probability in DOR-APV protocol.

Therefore, besides formula (6), the joint outage probability of SOR-AP(V) protocols can be obtained as:

$$\begin{aligned}
&\Pr\left(S\tilde{R}_{out,l}\right) \\
&\quad = \Pr^{l}\left\{\log_2\left(1+\gamma\omega_{S\tilde{R}}\right)<r\right\} \\
&\quad = \Pr^{l}\left\{\omega_{S\tilde{R}}<a_1\right\} = F^{l}_{\omega_{S\tilde{R}}}(a_1) \qquad (7)\\
&\Pr\left(S\tilde{R}D_{out,l}\right) \\
&\quad = \Pr^{T_{\tilde{R}}}\left\{\log_2\left(1+\gamma\omega_{SD}\right)<r\right\} \\
&\qquad \cdot\Pr^{(l-T_{\tilde{R}})}\left\{\log_2\left(1+\gamma\omega_{\tilde{R}D}\right)<r\right\} \\
&\quad = \Pr^{T_{\tilde{R}}}\left\{\omega_{SD}<a_1\right\}\cdot\Pr^{(l-T_{\tilde{R}})}\left\{\omega_{\tilde{R}D}<a_1\right\} \\
&\quad = F^{T_{\tilde{R}}}_{\omega_{SD}}(a_1)\,F^{(l-T_{\tilde{R}})}_{\omega_{\tilde{R}D}}(a_1) \qquad (8)\\
&\Pr\left(T_{\tilde{R}}=t\right) \\
&\quad = \Pr\left(S\tilde{R}_{out,t-1}\right)-\Pr\left(S\tilde{R}_{out,t}\right) \\
&\quad = F^{(t-1)}_{\omega_{S\tilde{R}}}(a_1)\left[1-F_{\omega_{S\tilde{R}}}(a_1)\right] \qquad (9)
\end{aligned}$$

where $T_i, i \in (AP, V, D)$ represents that node i decodes the data frame successfully in the T_ith ARQ round. We assume that $\tilde{R}$ can correctly decode the data frame in the subsequent ARQ rounds once it decodes the frame successfully in the $T_{\tilde{R}}$th ARQ round and it refuses to receive the frame from S when it still fails to decode the frame until the Lth ARQ round, i.e., both T_{AP} and T_V are independent RVs in the range of $[1, L-1]$, while T_D is a RV in the range of $[1, L]$.

C. DOR-APV PROTOCOL

Different from the SOR-AP(V) protocols which only need to study the transmission behavior of three data links S-D, S-$\tilde{R}$ and S-$\tilde{R}$-D, in the four-node system model established for DOR-APV protocol where both AP and V are selected as the optimal relays, it is necessary to add the study of link AP-V (V-AP). In other words, the outage probability of communication links between relays AP and V need to be specifically calculated in this protocol, which undoubtedly makes the calculation more complex. After analysis, there occur some cooperative subevents in the DOR-APV protocol according to the different value relations between RVs T_{AP}, T_V with value range in $[1, L-1]$ and RV T_D with value range in $[1, L]$. For concision, these cooperative subevents are summarized in Figure 5.

From Figure 5, there are mainly three possible cooperative subevents, i.e., No-relay cooperative subevent, Single-relay cooperative subevent and Dual-relay cooperative subevent, in the DOR-APV protocol. These three cooperative subevents together constitute the complete event group of DOR-APV protocol. In addition, each cooperative subevent also contains its own corresponding conditional subevents.

1) NO-RELAY COOPERATIVE SUBEVENT

This subevent indicates that no matter whether D can decode the data frame correctly or not, neither AP nor V can successfully decode the frame before D, and all T_D retransmissions are performed only by S. That is, if D decodes the data frame successfully in the ith ARQ round, this subevent can be expressed as:

$$\begin{cases} T_{AP}=T_V=T_D=i, & 1\le i\le L-1 \\ T_{AP}=T_V=L-1, & i=L. \end{cases}$$

Its operational example is shown in Figure 6, where $L=5$ and $T_{AP}=T_V=T_D=4$. Obviously, only $\Pr\left(SD_{out,l}\right)$, $\Pr\left(SAP_{out,l}\right)$ and $\Pr\left(SV_{out,l}\right)$ need to be considered in this subevent.

2) SINGLE-RELAY COOPERATIVE SUBEVENT

This subevent indicates no matter whether D can decode the frame correctly or not, either AP or V can successfully decode

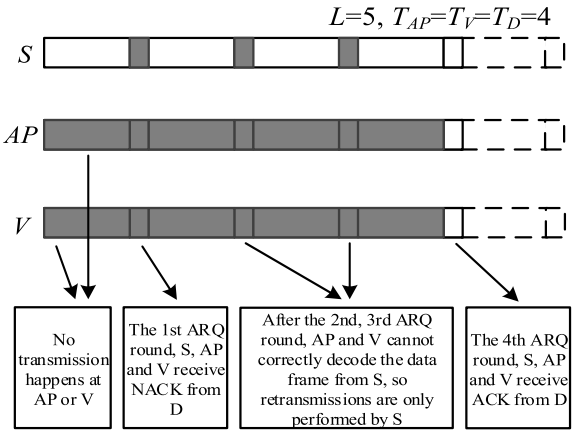

FIGURE 6. An operational example of No-relay cooperative subevent.

the frame before D, and all T_D retransmissions are performed jointly by this single relay and S. That is, assuming that D decodes the data frame successfully in the

ith ARQ round, this subevent can be expressed as two conditional subevents:

$$\begin{cases} T_{AP} < T_V = T_D = i, & 1 \le i \le L-1 \\ T_{AP} < T_V = L-1, & i = L. \end{cases}$$

(retransmissions are performed by S and AP) and

$$\begin{cases} T_V < T_{AP} = T_D = i, & 1 \le i \le L-1 \\ T_V < T_{AP} = L-1, & i = L \end{cases}$$

(retransmissions are performed by S and V). Taking the former as an example, its operational example is shown in Figure7.

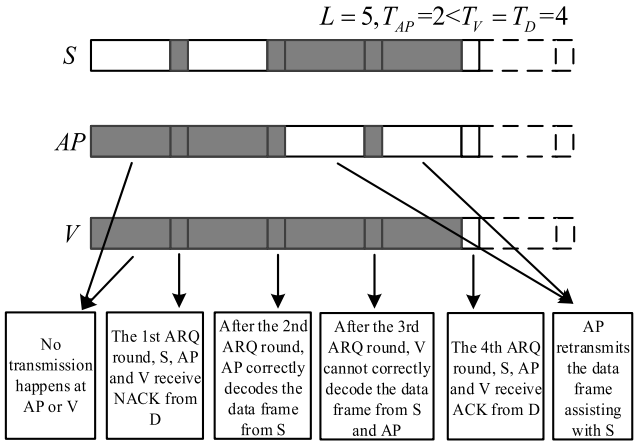

FIGURE 7. A example of Single-relay cooperative subevent.

Based on the outage probability of No-relay cooperative subevent and $\Pr\left(SAPD_{out,l}\right)$, $\Pr\left(SVD_{out,l}\right)$. $\Pr\left(SAPV_{out,l}\right)$ and $\Pr\left(SVAP_{out,l}\right)$ need to be considered in this subevent:

$$\begin{aligned} &\Pr\left(SAPV_{out,l}\right) \\ &= \Pr^{T_{AP}}\left\{\log_2\left(1+\gamma\omega_{SV}\right) < r\right\} \\ &\quad \cdot \Pr^{(l-T_{AP})}\left\{\log_2\left(1+\gamma\omega_{APV}\right) < r\right\} \\ &= \Pr^{T_{AP}}\left\{\omega_{SV} < a_1\right\} \cdot \Pr^{(l-T_{AP})}\left\{\omega_{APV} < a_1\right\} \\ &= F^{T_{AP}}_{\omega_{SV}}\left(a_1\right) F^{(l-T_{AP})}_{\omega_{APV}}\left(a_1\right) \end{aligned} \tag{10}$$

$$\begin{aligned} &\Pr\left(SVAP_{out,l}\right) \\ &= \Pr^{T_V}\left\{\log_2\left(1+\gamma\omega_{SAP}\right) < r\right\} \\ &\quad \cdot \Pr^{(l-T_V)}\left\{\log_2\left(1+\gamma\omega_{VAP}\right) < r\right\} \\ &= \Pr^{T_V}\left\{\omega_{SAP} < a_1\right\} \cdot \Pr^{(l-T_V)}\left\{\omega_{VAP} < a_1\right\} \\ &= F^{T_V}_{\omega_{SAP}}\left(a_1\right) F^{(l-T_V)}_{\omega_{VAP}}\left(a_1\right) \end{aligned} \tag{11}$$

3) DUAL-RELAY COOPERATIVE SUBEVENT

This subevent indicates that no matter whether D can decode the data frame correctly or not, both AP and V can successfully decode the data frame before D, and all T_D retransmissions are performed jointly by both of them and S. That is, assuming that D decodes the data frame successfully in the ith ARQ round, this subevent can be divided into three conditional subevents according to the different sequences that AP and V successfully decode the frame, which are denoted as conditional subevent A_1: AP and V decode the data frame synchronously

$$\left(\begin{cases} T_{AP} = T_V < T_D = i, 1 \le i \le L-1 \\ T_{AP} = T_V < L-1, i = L \end{cases}\right),$$

conditional subevent A_2: AP and V decode the data frame asynchronously and AP succeeds before

$$\mathrm{V}\left(\begin{cases} T_{AP} < T_V < T_D = i, 1 \le i \le L-1 \\ T_{AP} < T_V < L-1, i = L \end{cases}\right),$$

and conditional subevent A_3: AP and V decode the data frame asynchronously and V succeeds before

$$\mathrm{AP}\left(\begin{cases} T_V < T_{AP} < T_D = i, 1 \le i \le L-1 \\ T_V < T_{AP} < L-1, i = L \end{cases}\right).$$

Obviously, conditional subevents A_2 and A_3 are essentially identical, so taking conditional subevents A_1 and A_2 as examples, their operational examples are shown in Figure 8, respectively.

Besides all the above outage probability, the transmission behavior of link S-APV-D which represents both AP and V assist S in retransmitting frame to D needs to be considered in this subevent. After analysis, the joint outage probability of link S-APV-D under the above three conditional subevents can be expressed as shown in formulas (12)-(14), respectively.

To sum up, the outage probability expressions of each link in the four protocols are summarized in Table 2.

$$\begin{aligned} &\Pr\left(SA_1D_{out,l}\right) \\ &= \Pr^{T_{AP}}\left\{\log_2\left(1+\gamma\omega_{SD}\right) < r\right\} \\ &\quad \cdot \Pr^{(l-T_{AP})}\left\{\log_2\left(1+\gamma\omega_{APD}+\gamma\omega_{VD}\right) < r\right\} \\ &= F^{T_{AP}}_{\omega_{SD}}\left(a_1\right) F^{(l-T_{AP})}_{\omega_{APD}+\omega_{VD}}\left(a_1\right) \end{aligned} \tag{12}$$

$$\begin{aligned} &\Pr\left(SA_2D_{out,l}\right) \\ &= \Pr^{T_{AP}}\left\{\log_2\left(1+\gamma\omega_{SD}\right) < r\right\} \\ &\quad \cdot \Pr^{(T_V-T_{AP})}\left\{\log_2\left(1+\gamma\omega_{APD}\right) < r\right\} \\ &\quad \cdot \Pr^{(l-T_V)}\left\{\log_2\left(1+\gamma\omega_{APD}+\gamma\omega_{VD}\right) < r\right\} \\ &= F^{T_{AP}}_{\omega_{SD}}\left(a_1\right) F^{(T_V-T_{AP})}_{\omega_{APD}}\left(a_1\right) F^{(l-T_V)}_{\omega_{APD}+\omega_{VD}}\left(a_1\right) \end{aligned} \tag{13}$$

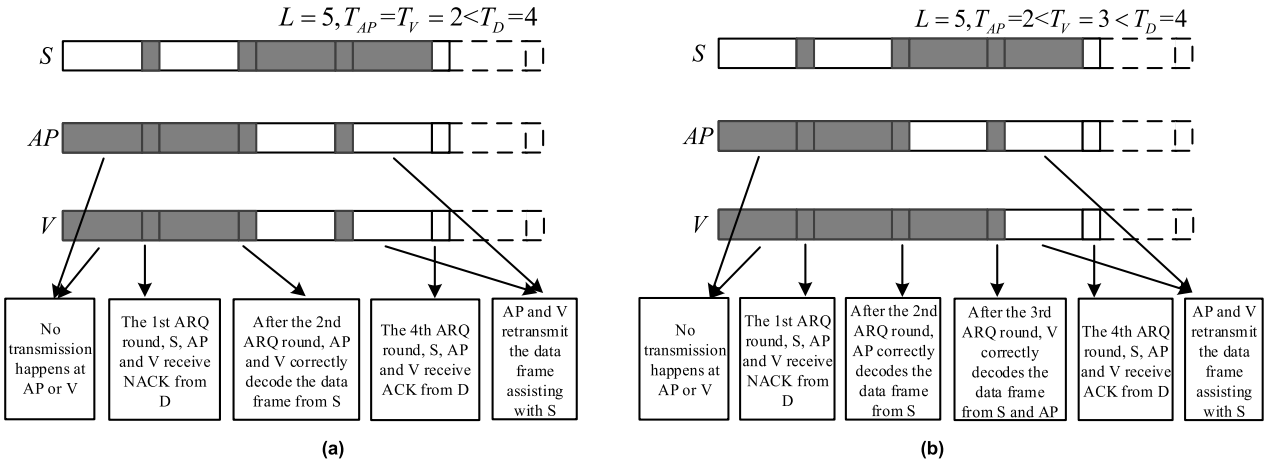

FIGURE 8. Operational examples of Dual-relay cooperative subevent seen by D. (a) Conditional subevent A_1 (b) Conditional subevent A_2.

TABLE 2. Joint outage probability of links in four protocols.

Link	Protocol			
	Non-OR ($N=0$)	SOR-AP ($N=1$)	SOR-V ($N=1$)	DOR-APV ($N=2$)
S-D	$F^{l}_{\omega_{SD}}(a_1)$	$F^{l}_{\omega_{SD}}(a_1)$	$F^{l}_{\omega_{SD}}(a_1)$	$F^{l}_{\omega_{SD}}(a_1)$
S-AP	-	$F^{l}_{\omega_{SAP}}(a_1)$	-	$F^{l}_{\omega_{SAP}}(a_1)$
S-AP-D	-	$F^{T_{AP}}_{\omega_{SD}}(a_1)F^{(l-T_{AP})}_{\omega_{APD}}(a_1)$	-	$F^{T_{AP}}_{\omega_{SD}}(a_1)F^{(l-T_{AP})}_{\omega_{APD}}(a_1)$
S-V	-	-	$F^{l}_{\omega_{SV}}(a_1)$	$F^{l}_{\omega_{SV}}(a_1)$
S-V-D	-	-	$F^{T_V}_{\omega_{SD}}(a_1)F^{(l-T_V)}_{\omega_{VD}}(a_1)$	$F^{T_V}_{\omega_{SD}}(a_1)F^{(l-T_V)}_{\omega_{VD}}(a_1)$
S-AP-V (S-V-AP)	-	-	-	$F^{T_{AP}}_{\omega_{SV}}(a_1)F^{(l-T_{AP})}_{\omega_{APV}}(a_1)$ $\left(F^{T_V}_{\omega_{SAP}}(a_1)F^{(l-T_V)}_{\omega_{VAP}}(a_1)\right)$
S-APV-D	-	-	-	$\begin{cases} F^{T_{AP}}_{\omega_{SD}}(a_1)F^{(l-T_{AP})}_{\omega_{APD}+\omega_{VD}}(a_1) \\ F^{T_{AP}}_{\omega_{SD}}(a_1)F^{(T_V-T_{AP})}_{\omega_{APD}}(a_1)F^{(l-T_V)}_{\omega_{APD}+\omega_{VD}}(a_1) \\ F^{T_V}_{\omega_{SD}}(a_1)F^{(T_{AP}-T_V)}_{\omega_{VD}}(a_1)F^{(l-T_{AP})}_{\omega_{APD}+\omega_{VD}}(a_1) \end{cases}$

$$\begin{aligned}
&\Pr\left(SA_3D_{out,l}\right) \\
&\quad=\Pr^{T_V}\left\{\log_2\left(1+\gamma\omega_{SD}\right)<r\right\} \\
&\qquad\cdot\Pr^{(T_{AP}-T_V)}\left\{\log_2\left(1+\gamma\omega_{VD}\right)<r\right\} \\
&\qquad\cdot\Pr^{(l-T_{AP})}\left\{\log_2\left(1+\gamma\omega_{APD}+\gamma\omega_{VD}\right)<r\right\} \\
&\quad=F^{T_V}_{\omega_{SD}}(a_1)\,F^{(T_{AP}-T_V)}_{\omega VD}(a_1)\,F^{(l-T_{AP})}_{\omega_{APD}+\omega_{VD}}(a_1) \qquad (14)
\end{aligned}$$

IV. MARKOV MODEL ESTABLISHMENT AND STATE TRANSITION PROBABILITY ANALYSIS

In order to study and compare the system performance of the four proposed protocols, a generalized 2-dimensional DTMC model, shown in Figure 9, is established for the four protocols, and the corresponding one-step state transition probability of each protocol is obtained, respectively.

In the novel DTMC model shown in Figure 9, state S represents that D decodes the data frame correctly, state F represents that D has not ever decoded the data frame successfully when all L ARQ rounds are exhausted and state

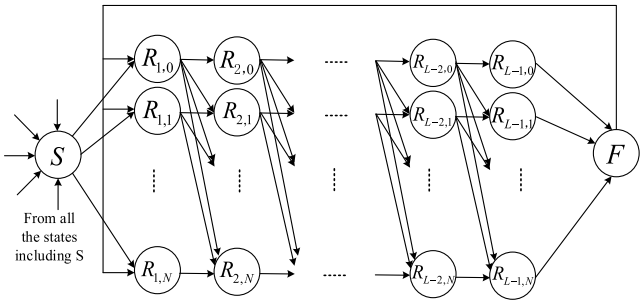

FIGURE 9. A generalized 2-dimensional DTMC model for four protocols.

$R_{i,j}\,(1\le i\le L-1, 0\le j\le N)$ represents that there are j (of N) relays successfully decode the data frame but D fails to decode the frame in the ith ARQ round.

Moreover, there are totally $(L-1)(N+1)+2$ states in this DTMC. Because the four protocols are represented by

TABLE 3. One-step state transition probability of DTMC model for SOR-AP(V) protocol.

Transition situation	Start state	Destination state	Transition probability	Condition
Link S-D is successful in 1st round	S / F	S	$1\text{-}\Pr\left(SD_{out,1}\right)$	-
Links S-D, S- $\tilde{R}$ are failed in 1st round	S / F	$R_{1,0}$	$\Pr\left(SD_{out,1}\right)\cdot\Pr\left(S\tilde{R}_{out,1}\right)$	-
S-D is failed, but S- $\tilde{R}$ is successful in 1st round	S / F	$R_{1,1}$	$\Pr\left(SD_{out,1}\right)\cdot\left[1-\Pr\left(S\tilde{R}_{out,1}\right)\right]$	-
S-D is successful in (i+1)th round	$R_{i,0}$	S	$1\text{-}\Pr\left(SD_{out,i+1}\mid SD_{out,i}\right)$	$1\le i\le L-1$
S-D, S- $\tilde{R}$ are failed in (i+1)th round	$R_{i,0}$	$R_{i+1,0}$	$\Pr\left(SD_{out,i+1}\mid SD_{out,i}\right)\cdot\Pr\left(S\tilde{R}_{out,i+1}\mid S\tilde{R}_{out,i}\right)$	$1\le i\le L-2$
S-D is failed, but S- $\tilde{R}$ is successful in (i+1)th round	$R_{i,0}$	$R_{i+1,1}$	$\Pr\left(SD_{out,i+1}\mid SD_{out,i}\right)\cdot\left[1-\Pr\left(S\tilde{R}_{out,i+1}\mid S\tilde{R}_{out,i}\right)\right]$	$1\le i\le L-2$
S-D, S- $\tilde{R}$ are failed in Lth round	$R_{i,0}$	F	$\Pr\left(SD_{out,i+1}\mid SD_{out,i}\right)$	$i=L-1$
S- $\tilde{R}$ -D is successful in (i+1)th round	$R_{i,1}$	S	$1\text{-}\Pr\left(S\tilde{R}D_{out,i+1}\mid S\tilde{R}D_{out,i}\right)$	$1\le i\le L-1$
S- $\tilde{R}$ -D is failed in (i+1)th round	$R_{i,1}$	$R_{i+1,1}$	$\Pr\left(S\tilde{R}D_{out,i+1}\mid S\tilde{R}D_{out,i}\right)$	$1\le i\le L-2$
S- $\tilde{R}$ -D is failed in Lth round	$R_{i,1}$	F	$\Pr\left(S\tilde{R}D_{out,i+1}\mid S\tilde{R}D_{out,i}\right)$	$i=L-1$

different values of N, the one-step state transition probability of four protocols needs to be discussed separately.

A. NON-OR PROTOCOL

When $N=0$, the 2-dimensional DTMC in Figure 9 can be simplified to the 1-dimensional model shown in Figure 10.

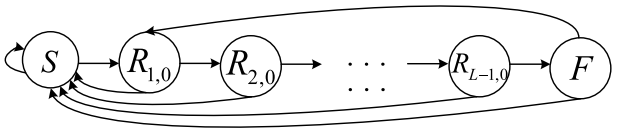

FIGURE 10. The simplified 1-dimensional DTMC model for Non-OR protocol.

It can be clearly seen from Figure10 that there are totally $L+1$ states in this DTMC, and its one-step state transition probability can be easily obtained as formula (15).

$$\begin{cases}\Pr_{SS}=\Pr_{FS}=1\text{-}\Pr\left(SD_{out,1}\right)\\ \Pr_{SR_{1,0}}=\Pr_{FR_{1,0}}=\Pr\left(SD_{out,1}\right)\\ \Pr_{R_{i,0}R_{i+1,0}}=\Pr\left(SD_{out,i+1}|SD_{out,i}\right), & 1\le i\le L-2\\ \Pr_{R_{i,0}S}=1-\Pr\left(SD_{out,i+1}|SD_{out,i}\right), & 1\le i\le L-1\\ \Pr_{R_{L-1,0}F}=\Pr\left(SD_{out,L}|SD_{out,L-1}\right)\end{cases} \tag{15}$$

B. SOR-AP(V) PROTOCOL

A 2-dimensional DTMC for SOR-AP(V) protocol can be established in Figure 11 by making $N=1$ in Figure 9. There are totally $2L$ states in this DTMC and its one-step state transition probability is summarized in Table 3.

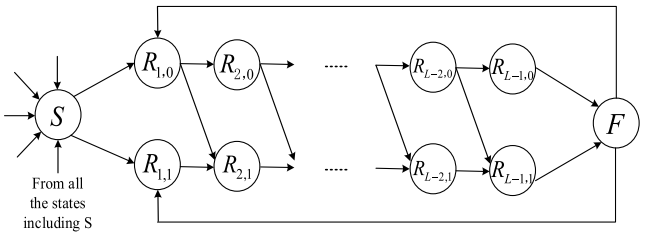

FIGURE 11. The 2-dimensional DTMC model for SOR-AP(V) protocol.

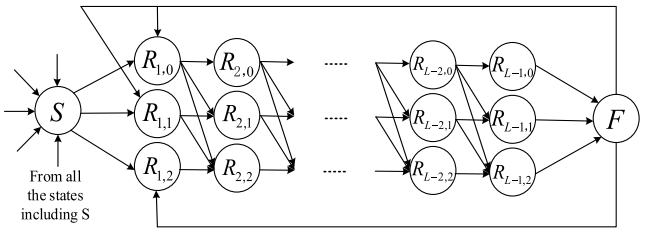

FIGURE 12. The 2-dimensional DTMC model for SOR-AP(V) protocol.

C. DOR-APV PROTOCOL

Similarly, the DTMC for DOR-APV protocol can be obtained in Figure 12 when $N=2$, and this model totally has $3L-1$ states. Now, we can compare the total number of states in three DTMCs built for the four protocols by summarizing them in the Table 4 , and it can be seen form Table 4 that the larger the maximum transmission number L is, the higher the computational complexity will be, and the DTMC for DOR-APV protocol has the most number of states under the same L.

According to the analysis in Section III, the expressions of one-step state transition probability of the 2-dimensional

TABLE 4. A comparison of total number of states between three DTMCs.

State number	L							
	1	2	3	4	5	6	7	8
Figure 10	2	3	4	5	6	7	8	9
Figure 11	2	4	6	8	10	12	14	16
Figure 12	2	5	8	11	14	17	20	23

DTMC model for DOR-APV protocol can be obtained by using the calculated outage probability in Table 2. To be specific, there are four types of transition:

1) THE TRANSITION FROM THE INITIAL STATE S/F

The state S or state F representing a successful or failed transmission of the previous data frame can only move to state S, $R_{1,0}$, $R_{1,1}$, or $R_{1,2}$ in the first round, which show the situations that in the first ARQ round, D decodes the frame correctly; both AP, V and D cannot decode the frame; only a single relay (AP or V) successfully decodes the data frame but D does not decode the frame; both AP and V decode the frame while D fails to decode the frame, respectively. The corresponding transition probability is:

$$\begin{aligned}&\Pr_{SS}\\&= \Pr_{FS} = 1-\Pr\left(SD_{out,1}\right)\end{aligned} \tag{16}$$

$$\begin{aligned}&\Pr_{SR_{1,0}}\\&= \Pr_{FR_{1,0}} = \Pr\left(SD_{out,1}\right)\cdot\Pr\left(SAP_{out,1}\right)\cdot\Pr\left(SV_{out,1}\right)\end{aligned} \tag{17}$$

$$\begin{aligned}&\Pr_{SR_{1,1}}\\&= \Pr_{FR_{1,1}} = \Pr\left(SD_{out,1}\right)\cdot\left[\Pr\left(SAP_{out,1}\right)\left(1-\Pr\left(SV_{out,1}\right)\right)\right.\\&\quad\left.+\Pr\left(SV_{out,1}\right)\left(1-\Pr\left(SAP_{out,1}\right)\right)\right]\end{aligned} \tag{18}$$

$$\begin{aligned}&\Pr_{SR_{1,2}}\\&= \Pr_{FR_{1,2}} = \Pr\left(SD_{out,1}\right)\cdot\left[1-\Pr\left(SAP_{out,1}\right)\right]\\&\quad\cdot\left[1-\Pr\left(SV_{out,1}\right)\right]\end{aligned} \tag{19}$$

2) THE TRANSITION FROM THE GENERAL STATE $R_{i,0}$ OF NO-RELAY COOPERATIVE SUBEVENT

The state $R_{i,0}$ representing a retransmission without relay cooperation in the ith ARQ round can move to state S, $R_{i+1,0}$, $R_{i+1,1}$, $R_{i+1,2}$, or F (only when $i = L-1$) in the next round, which show the situations that in the $(i+1)$th ARQ round, D decodes the frame correctly; both AP, V and D cannot decode the frame; only a single relay (AP or V) successfully decodes the data frame but D does not decode the frame; both AP and V decode the frame while D fails to decode the frame; and D finally fails to decode the data frame and discards it when all the ARQ rounds are exhausted, respectively. Their transition probability is:

$$\begin{aligned}&\Pr_{R_{i,0}S}\\&= 1-\Pr\left(SD_{out,i+1}|SD_{out,i}\right),\quad 1\le i\le L-1\end{aligned} \tag{20}$$

$$\begin{aligned}&\Pr_{R_{i,0}R_{i+1,0}}\\&= \Pr\left(SD_{out,i+1}|SD_{out,i}\right)\cdot\Pr\left(SAP_{out,i+1}|SAP_{out,i}\right)\\&\quad\cdot\Pr\left(SV_{out,i+1}|SV_{out,i}\right),\quad 1\le i\le L-2\end{aligned} \tag{21}$$

$$\begin{aligned}&\Pr_{R_{i,0}R_{i+1,1}}\\&= \Pr\left(SD_{out,i+1}|SD_{out,i}\right)\\&\quad\cdot\left\{\Pr\left(SAP_{out,i+1}|SAP_{out,i}\right)\left[1-\Pr\left(SV_{out,i+1}|SV_{out,i}\right)\right]\right.\\&\quad\left.+\Pr\left(SV_{out,i+1}|SV_{out,i}\right)\left[1-\Pr\left(SAP_{out,i+1}|SAP_{out,i}\right)\right]\right\},\\&\qquad 1\le i\le L-2\end{aligned} \tag{22}$$

$$\begin{aligned}&\Pr_{R_{i,0}R_{i+1,2}}\\&= \Pr\left(SD_{out,i+1}|SD_{out,i}\right)\cdot\left[1-\Pr\left(SAP_{out,i+1}|SAP_{out,i}\right)\right]\\&\quad\cdot\left[1-\Pr\left(SV_{out,i+1}|SV_{out,i}\right)\right],\quad 1\le i\le L-2\end{aligned} \tag{23}$$

$$\begin{aligned}&\Pr_{R_{L-1,0}F}\\&= \Pr\left(SD_{out,L}|SD_{out,L-1}\right)\end{aligned} \tag{24}$$

3) THE TRANSITION FROM THE GENERAL STATE $R_{i,1}$ OF SINGLE-RELAY COOPERATIVE SUBEVENT

Similarly, the state $R_{i,1}$ representing a retransmission with single-relay cooperation in the ith ARQ round can move to state S, $R_{i+1,1}$, $R_{i+1,2}$, or F (only when $i = L-1$) in the next round, which show the situations that in the $(i+1)$th ARQ round, D decodes the frame correctly; D and the other relay cannot decode the frame; the other relay decodes the frame but D fails to decode it; and D finally fails to decode the data frame and discards it when L is reached, respectively. It is worth noting that, as mentioned before, there are two simple conditional subevents (i.e., either AP or V assists S in retransmitting the data frame to D) which constitute the complete event group of single-relay cooperation and both of them are incompatible and positive probability. We denote the probability of single-relay cooperation as $\Pr\left(one-relay\right)$. It is obvious that:

$$\Pr\left(one-relay\right)=\Pr\left(AP,\,one-relay\right)+\Pr\left(V,\,one-relay\right)$$

where $\Pr\left(AP,\,one-relay\right)$ ($\Pr\left(V,\,one-relay\right)$) is the joint probability that it is the relay AP(V) who decodes the data frame successfully and retransmits it in the single-relay cooperative event.

It can be calculated as formula (25):

$$\begin{cases}\Pr\left(AP,\,one-relay\right)=\sum_{t=1}^{L-1}\Pr\left(T_{AP}=t\right)\Pr\left(SAPV_{out,L-1}\right)\\ \Pr\left(V,\,one-relay\right)=\sum_{t=1}^{L-1}\Pr\left(T_{V}=t\right)\Pr\left(SVAP_{out,L-1}\right)\end{cases} \tag{25}$$

and based on it, we can easily obtain the corresponding conditional probability as shown in formula (26), as shown at the bottom of the page.

Obviously, $\Pr(AP|one-relay)+\Pr(V|one-relay)=1$. Therefore, the transition probability expressions of state $R_{i,1}$ can be expressed as formulas (27)-(30), respectively.

$$\begin{aligned}&\Pr_{R_{i,1}S}\\&=\Pr(AP|one-relay)\left[1-\Pr\left(SAPD_{out,i+1}|SAPD_{out,i}\right)\right]\\&\quad+\Pr(V|one-relay)\left[1-\Pr\left(SVD_{out,i+1}|SVD_{out,i}\right)\right],\\&\qquad 1\le i\le L-1\end{aligned}\tag{27}$$

$$\begin{aligned}&\Pr_{R_{i,1}R_{i+1,1}}\\&=\Pr(AP|one-relay)\Pr\left(SAPD_{out,i+1}|SAPD_{out,i}\right)\\&\quad\cdot\Pr\left(SAPV_{out,i+1}|SAPV_{out,i}\right)\\&\quad+\Pr(V|one-relay)\Pr\left(SVD_{out,i+1}|SVD_{out,i}\right)\\&\quad\cdot\Pr\left(SVAP_{out,i+1}|SVAP_{out,i}\right),\quad 1\le i\le L-2\end{aligned}\tag{28}$$

$$\begin{aligned}&\Pr_{R_{i,1}R_{i+1,2}}\\&=\Pr(AP|one-relay)\Pr\left(SAPD_{out,i+1}|SAPD_{out,i}\right)\\&\quad\cdot\left[1-\Pr\left(SAPV_{out,i+1}|SAPV_{out,i}\right)\right]\\&\quad+\Pr(V|one-relay)\Pr\left(SVD_{out,i+1}|SVD_{out,i}\right)\\&\quad\cdot\left[1-\Pr\left(SVAP_{out,i+1}|SVAP_{out,i}\right)\right],\quad 1\le i\le L-2\end{aligned}\tag{29}$$

$$\begin{aligned}&\Pr_{R_{L-1,1}F}\\&=\Pr(AP|one-relay)\Pr\left(SAPD_{out,L}|SAPD_{out,L-1}\right)\\&\quad+\Pr(V|one-relay)\Pr\left(SVD_{out,L}|SVD_{out,L-1}\right)\end{aligned}\tag{30}$$

4) THE TRANSITION FROM THE GENERAL STATE $R_{i,2}$ OF DUAL-RELAY COOPERATIVE SUBEVENT

The state $R_{i,2}$ representing a retransmission with dual-relay cooperation in the ith ARQ round can move to state S, $R_{i+1,2}$, or F (only when $i=L-1$) in the next round, which show the situations that in the $(i+1)$th ARQ round, D decodes the frame correctly; D fails to decode the frame; and D finally discards the data frame in the last ARQ round. Similarly, as described in Section III, the three incompatible conditional subevents: A_1, A_2 and A_3, which are all positive probability, jointly constitute the complete event group of dual-relay cooperation, we also denote the probability of dual-relay cooperation as $\Pr(two-relay)$. It is obvious that:

$$\Pr(two-relay)=\sum_{k=1}^{3}\Pr(A_k,two-relay)$$

where $\Pr(A_k,two-relay)$ is the joint probability that it is the conditional subevent A_k that occurs in the dual-relay cooperative subevent, and it can be calculated as:

$$\begin{aligned}&\Pr(A_1,two-relay)\\&=\sum_{t=1}^{L-1}\Pr(T_{AP}=T_V=t)=\sum_{t=1}^{L-1}\Pr(T_{AP}=t)\Pr(T_V=t)\end{aligned}\tag{31}$$

$$\begin{aligned}&\Pr(A_2,two-relay)\\&=\Pr(T_{AP}=t_1<T_V=t_2)\\&=\sum_{t_1=1}^{L-2}\Pr(T_{AP}=t_1)\sum_{t_2=t_1+1}^{L-1}\left[\Pr\left(SAPV_{out,t_2-1}\right)\right.\\&\quad\left.-\Pr\left(SAPV_{out,t_2}\right)\right]\end{aligned}\tag{32}$$

$$\begin{aligned}&\Pr(A_3,two-relay)\\&=\Pr(T_V=t_2<T_{AP}=t_1)\\&=\sum_{t_2=1}^{L-2}\Pr(T_V=t_2)\sum_{t_1=t_2+1}^{L-1}\left[\Pr\left(SVAP_{out,t_1-1}\right)\right.\\&\quad\left.-\Pr\left(SVAP_{out,t_1}\right)\right]\end{aligned}\tag{33}$$

and its corresponding conditional probability can be expressed as:

$$\Pr(A_k|two-relay)=\frac{\Pr(A_k,two-relay)}{\sum_{k=1}^{3}\Pr(A_k,two-relay)},\quad k=1,2,3\tag{34}$$

It is obvious that $\sum_{k=1}^{3}\Pr(A_k|two-relay)=1$. Therefore, the transition probability expressions of state $R_{i,2}$ can be

$$\begin{cases}\Pr(AP|one-relay)\\=\dfrac{\sum_{t=1}^{L-1}\Pr(T_{AP}=t)\Pr\left(SAPV_{out,L-1}\right)}{\sum_{t=1}^{L-1}\left[\Pr(T_{AP}=t)\Pr\left(SAPV_{out,L-1}\right)+\Pr(T_V=t)\Pr\left(SVAP_{out,L-1}\right)\right]}\\\Pr(V|one-relay)\\=\dfrac{\sum_{t=1}^{L-1}\Pr(T_V=t)\Pr\left(SVAP_{out,L-1}\right)}{\sum_{t=1}^{L-1}\left[\Pr(T_{AP}=t)\Pr\left(SAPV_{out,L-1}\right)+\Pr(T_V=t)\Pr\left(SVAP_{out,L-1}\right)\right]}\end{cases}\tag{26}$$

expressed as:

$$\begin{aligned}&\Pr_{R_{i,2}S}\\&=\sum_{k=1}^{3}\Pr\left(A_k|two-relay\right)\\&\cdot\left[1-\Pr\left(SA_kD_{out,i+1}|SA_kD_{out,i}\right)\right],\quad 1\le i\le L-1\end{aligned}\tag{35}$$

$$\begin{aligned}&\Pr_{R_{i,2}R_{i+1,2}}\\&=\sum_{k=1}^{3}\Pr\left(A_k|two-relay\right)\\&\cdot\Pr\left(SA_kD_{out,i+1}|SA_kD_{out,i}\right),\quad 1\le i\le L-2\end{aligned}\tag{36}$$

$$\begin{aligned}&\Pr_{R_{L-1,2}F}\\&=\sum_{k=1}^{3}\Pr\left(A_k|two-relay\right)\cdot\Pr\left(SA_kD_{out,L}|SA_kD_{out,L-1}\right)\end{aligned}\tag{37}$$

From the above, we can get all the one-step state transition probability of the four proposed protocols, and they will be used in the subsequent system performance analysis.

V. SYSTEM PERFORMANCE ANALYSIS OF FOUR PROTOCOLS

Based on the one-step state transition probability obtained in Section IV, this section devotes to derive the closed-form expressions of system performance including throughput and energy efficiency.

A. SYSTEM THROUGHPUT

The system throughput defined in this paper is the average number of data frames successfully received by D within one time slot, which equals to the average number of time slots consumed by the DTMC in the state S, i.e., the steady state probability of state S. Supposing that the steady state distribution of the generalized DTMC model is $\pi=(\pi_S,\pi_1,\cdots,\pi_F)$ where π_S is the steady probability of state S, then the system throughput can be calculated by using $\pi P=\pi$ and $\sum\pi=1$, where P is the state transition probability matrix of each protocol. The closed expression of system throughput under arbitrary maximum transmission number L for four protocols (N) can be obtained as follows:

$$\pi_S\left(L,N\right)=\frac{1-FER\left(L,N\right)}{1+f\left(L,N\right)}\tag{38}$$

where $FER\left(L,N\right)$ is the frame error rate (FER) and $f(L,N)$ is an undetermined function of L and N. They can be expressed as:

$$FER(L,N)\triangleq\begin{cases}\sum_{n_1=0}^{N}\Pr_{SR_{1,n_1}}\cdot\Pr_{R_{1,n_1}F},L=2\\\sum_{n_1=0}^{N}\Pr_{SR_{1,n_1}}\cdot\prod_{i=1}^{L-2}\left[\sum_{n_{i+1}=n_i}^{N}\Pr_{R_{i,n_i}R_{i+1,n_{i+1}}}\right]\\\quad\cdot\Pr_{R_{L-1,n_{L-1}}F},L\ge3\end{cases}\tag{39}$$

and

$$f(L,N)\triangleq\begin{cases}\sum_{n_1=0}^{N}\Pr_{SR_{1,n_1}},&L=2\\f(L-1,N)+\sum_{n_1=0}^{N}\Pr_{SR_{1,n_1}}\\\quad\cdot\prod_{i=1}^{L-2}\left[\sum_{n_{i+1}=n_i}^{N}\Pr_{R_{i,n_i}R_{i+1,n_{i+1}}}\right],&L\ge3\end{cases}\tag{40}$$

where n_i $(0\le n_i\le N)$ represents the number of relays successfully decoding the frame in the ith ARQ round.

Thus, the system throughput under arbitrary maximum transmission number L of proposed four protocols can be obtained by computing equations (39) and (40) and substituting them into (38).

B. ENERGY EFFICIENCY

The energy efficiency defined in this paper is the average number of data frames correctly transmitted by system within one time slot per energy (Joule). Denoting K(frames/s) as the average number of data frames transmitted in a time slot and $P_{avg}\left(L,N\right)$ is the average power consumption value per one data frame of four protocols (N) under L. The expression of energy efficiency $\eta\left(L,N\right)$ can be expressed as:

$$\eta\left(L,N\right)=K\cdot\frac{1-FER\left(L,N\right)}{P_{avg}\left(L,N\right)}\tag{41}$$

This paper uses a general power consumption model which considers the power consumption of all the amplifiers P_A and the power consumption of transmitter and receiver circuit blocks P_{ct} and P_{cr}, which can be expressed as:

$$\begin{cases}P_{ct}=P_{DAC}+P_{filt}+P_{mix}+P_{syn}\\P_{cr}=P_{filt}+P_{LNA}+P_{mix}+P_{IFA}+P_{ADC}+P_{syn}\end{cases}$$

where P_{DAC}, P_{filt}, P_{mix}, P_{syn}, P_{filr}, P_{LNA}, P_{IFA} and P_{ADC} are the power consumption values of the digital-to-analog converter, the filter, the mixer, the frequency synthesizer, the active filter at the receiver, the low-noise amplifier, the intermediate frequency amplifier and the analog-to-digital converter, respectively. Moreover, the power consumption used for transmitting and receiving feedback information (i.e., ANK and NACK) is ignored in this paper. Then the average power consumption for one data frame of the four proposed protocols can be expressed as:

$$P_{avg}\left(L,N\right)=\sum_{n=0}^{N}\bar{P}_n\left(L\right)\tag{42}$$

where $\bar{P}_n\left(L\right),0\le n\le N$ represents the average power consumption under n-relay cooperation. We denote $\Pr_i\left(T_{AP},T_V\right)$ as the probability that AP and V respectively decode the data frame correctly in the T_{AP}th and T_Vth ARQ round when the ARQ process is completed in the ith ARQ round, and $P_i\left(T_{AP},T_V\right)$ is its corresponding power consumption value.

Taking the most complex DOR-APV protocol as an example, the $\bar{P}_n(L)$ can be calculated respectively as follows:

1) The average power consumption under no-relay cooperation (i.e., $n=0$):

$$\bar{P}_0(L)=\sum_{i=1}^{L}\Pr_i(T_{AP}=i,T_V=i)\cdot P_i(T_{AP}=i,T_V=i),\quad L\geq 1 \tag{43}$$

where $\Pr_i(T_{AP}=i,T_V=i)$ and $P_i(T_{AP}=i,T_V=i)$ are given by formula (44) and (45):

$$\Pr_i(T_{AP}=i,T_V=i)=\begin{cases}1-\Pr\left(SD_{out,1}\right), & i=1\\ \left[\Pr\left(SD_{out,i-1}\right)-\Pr\left(SD_{out,i}\right)\right]\\ \cdot\Pr\left(SAP_{out,i-1}\right)\Pr\left(SV_{out,i-1}\right), & 2\leq i\leq L-1\\ \Pr\left(SD_{out,L-1}\right)\\ \quad\cdot\Pr\left(SAP_{out,L-1}\right)\Pr\left(SV_{out,L-1}\right), & i=L\end{cases} \tag{44}$$

$$P_i(T_{AP}=i,T_V=i)=\begin{cases}P_A+P_{ct}+3P_{cr}, & i=1\\ i\left(P_A+P_{ct}+3P_{cr}\right), & 2\leq i\leq L-1\\ LP_A+LP_{ct}+(3L-2)P_{cr}, & i=L\end{cases} \tag{45}$$

2) The average power consumption under single-relay cooperation (i.e., $n=1$):

As described in Section III, the complete event group of single-relay cooperation is composed of two conditional subevents, so the expression of $\bar{P}_1(L)$ can be obtained as:

$$\bar{P}_1(L)=\Pr(AP|one-relay)\,\bar{P}_{AP|one-relay}(L)+\Pr(V|one-relay)\,\bar{P}_{V|one-relay}(L),\quad L\geq 2 \tag{46}$$

where $\bar{P}_{AP|one-relay}(L)$ ($\bar{P}_{V|one-relay}(L)$) is the average power consumption under the condition of the single relay AP(V) decodes the data frame successfully and retransmits it, which can be expressed as:

$$\begin{cases}\bar{P}_{AP|one-relay}(L)=\sum_{i=2}^{L}\sum_{t=1}^{i-1}\Pr_i(T_{AP}=t,T_V=i)\cdot P_i(T_{AP}=t,T_V=i),\quad L\geq 2\\ \bar{P}_{V|one-relay}(L)=\sum_{i=2}^{L}\sum_{t=1}^{i-1}\Pr_i(T_V=t,T_{AP}=i)\cdot P_i(T_V=t,T_{AP}=i),\quad L\geq 2\end{cases} \tag{47}$$

Taking AP as an example, $\Pr_i(T_{AP}=t,T_V=i)$ and $P_i(T_{AP}=t,T_V=i)$ are shown as formulas (48) and (49).

$$\Pr_i(T_{AP}=t,T_V=i)=\begin{cases}\Pr(T_{AP}=t)\cdot\Pr\left(SAPV_{out,i-1}\right)\\ \cdot\left[\Pr\left(SAPD_{out,i-1}\right)\right.\\ \quad\left.-\Pr\left(SAPD_{out,i}\right)\right], & 2\leq i\leq L-1\\ \Pr(T_{AP}=t)\cdot\Pr\left(SAPV_{out,L-1}\right)\\ \quad\cdot\Pr\left(SAPD_{out,L-1}\right), & i=L\end{cases} \tag{48}$$

$$P_i(T_{AP}=t,T_V=i)=\begin{cases}iP_A+iP_{ct}+(2i+t)P_{cr}, & 2\leq i\leq L-1\\ LP_A+LP_{ct}+(2L+t-1)P_{cr}, & i=L\end{cases} \tag{49}$$

3) The average power consumption under dual-relay cooperation (i.e., $n=2$):

Similarly, the expression of $\bar{P}_2(L)$ can be obtained as:

$$\bar{P}_2(L)=\sum_{k=1}^{3}\Pr(A_k|two-relay)\cdot\bar{P}_{A_k|two-relay}(L),\quad L\geq 2 \tag{50}$$

where $\bar{P}_{A_k|two-relay}(L)$ is the average power consumption under the condition of the dual-relay cooperation with subevent A_k, which needs to be discussed, separately.

$$\bar{P}_{A_1|two-relay}(L)=\sum_{i=2}^{L}\sum_{t=1}^{i-1}\Pr_i(T_{AP}=t,T_V=t)\cdot P_i(T_{AP}=t,T_V=t),\quad L\geq 2 \tag{51}$$

where $\Pr_i(T_{AP}=t,T_V=t)$ and $P_i(T_{AP}=t,T_V=t)$ can be expressed as:

$$\Pr_i(T_{AP}=t,T_V=t)=\begin{cases}\Pr(T_{AP}=t)\Pr(T_V=t)\left[\Pr\left(SA_1D_{out,i-1}\right)\right.\\ \quad\left.-\Pr\left(SA_1D_{out,i}\right)\right], & 2\leq i\leq L-1\\ \Pr(T_{AP}=t)\Pr(T_V=t)\cdot\Pr\left(SA_1D_{out,L-1}\right), & i=L\end{cases} \tag{52}$$

$$P_i(T_{AP}=t,T_V=t)=\begin{cases}(2i-t)P_A+(2i-t)P_{ct}+(2i+t)P_{cr}, & 2\leq i\leq L-1\\ (2L-t)P_A+(2L-t)P_{ct}+(2L+t)P_{cr}, & i=L\end{cases} \tag{53}$$

While $\bar{P}_{A_2|two-relay}(L)$

$$=\sum_{i=3}^{L}\sum_{t_1=1}^{i-2}\sum_{t_2=t_1+1}^{i-1}\Pr_i(T_{AP}=t_1,T_V=t_2)\cdot P_i(T_{AP}=t_1,T_V=t_2),\quad L\geq 3 \tag{54}$$

where $\Pr_i(T_{AP}=t_1,T_V=t_2)$ and $P_i(T_{AP}=t_1,T_V=t_2)$ are expressed as formula (55) and (56).

$$\Pr_i(T_{AP}=t_1,T_V=t_2)=\begin{cases}\Pr(T_{AP}=t_1)\cdot\left[\Pr\left(SAPV_{out,t_2-1}\right)-\Pr\left(SAPV_{out,t_2}\right)\right]\\ \cdot\left[\Pr\left(SA_2D_{out,i-1}\right)-\Pr\left(SA_2D_{out,i}\right)\right], & 3\leq i\leq L-1\\ \Pr(T_{AP}=t_1)\cdot\left[\Pr\left(SAPV_{out,t_2-1}\right)-\Pr\left(SAPV_{out,t_2}\right)\right]\\ \cdot\Pr\left(SA_2D_{out,L-1}\right), & i=L\end{cases} \tag{55}$$

$$P_i(T_{AP}=t_1,T_V=t_2)=\begin{cases}(2i-t_2)P_A+(2i-t_2)P_{ct}\\ \quad+(2i+t_1)P_{cr}, & 3\leq i\leq L-1\\ (2L-t_2)P_A+(2L-t_2)P_{ct}\\ \quad+(2L+t_1)P_{cr}, & i=L\end{cases} \tag{56}$$

TABLE 5. System parameters.

Parameter	Value	Parameter	Value
P_A	$1.3\times10^{-3}W$	r	$0.5bits/slot/Hz$
P_{ct}	$10^{-4}W$	d_{SD}	$[100,1000]m$
P_{cr}	$5\times10^{-5}W$	p_1, p_2	0.3 / 0.4 / 0.5 / 0.6
γ	$105dB$	q_1, q_2	0.6 / 0.7 / 0.8 / 0.9
β	4	K	$5 frames/s$

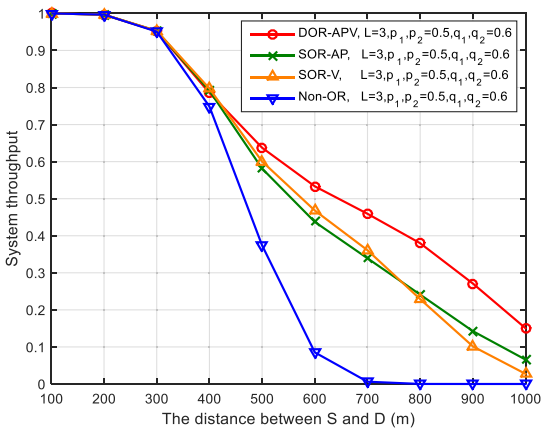

FIGURE 13. Study case 1: system throughput comparison of four proposed protocols.

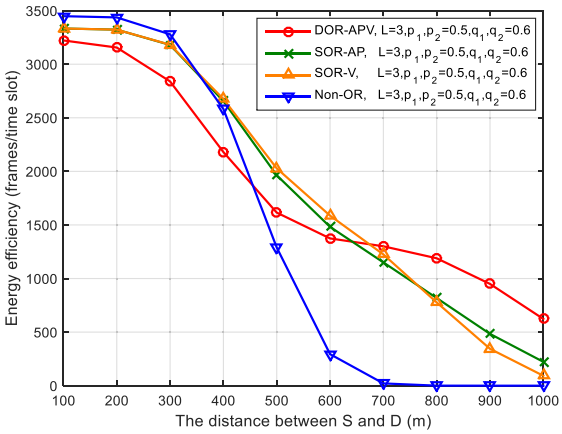

FIGURE 14. Study case 1: energy efficiency comparison of four proposed protocols.

Similarly, the calculation of $\bar{P}_{A_3|two-relay}(L)$ is same as that of $\bar{P}_{A_2|two-relay}(L)$, which is not repeated here. Finally, we can obtain the energy efficiency of DOR-APV protocol by calculating the formula (42)-(56) and substituting the results into (41). For brevity, the calculation of energy efficiency for other protocols is the same and not repeated here, too.

VI. SYSTEM PERFORMANCE SIMULATION AND EVALUATION

In this section, three study cases are executed by using MATLAB numerical simulation to compare the system performance of the four proposed protocols and evaluate the impact of network parameters on system performance. The parameters used in this paper are summarized in Table 5. Based on [35], $\gamma = 10\lg\left(\frac{P_t}{N_0}\right) = 10\lg\left(\frac{10^{-3}}{10^{-13.5}}\right) = 105dB$. $p_1(p_2)$ and $q_1(q_2)$ are the ratio of the distance from S to AP(V), i.e., $d_{SAP}(d_{SV})$ and the distance from AP(V) to D, i.e., $d_{APD}(d_{VD})$, to the distance from S to D, i.e., d_{SD}, respectively. That is:

$$p_1 = \frac{d_{SAP}}{d_{SD}}(p_2 = \frac{d_{SV}}{d_{SD}}),\ q_1 = \frac{d_{APD}}{d_{SD}}(q_2 = \frac{d_{VD}}{d_{SD}})$$

A. STUDY CASE 1: SYSTEM PERFORMANCE COMPARISON OF FOUR PROPOSED PROTOCOLS

In order to evaluate and compare the system performance of the four proposed protocols, the throughput and energy efficiency are simulated in Figure 13 and Figure 14 as a function of d_{SD} under different protocols, respectively. From them, it can be observed firstly that both throughput and energy efficiency deteriorate with the increase of d_{SD}, which is because that SNR at the receiver decreases with the increase of d_{SD}, resulting in the decline of performance.

Secondly, it can be seen from Figure 13 that the curve of DOR-APV protocol achieves the best throughput performance compared with other curves, this is because that the more the "helpers" are in the network, the more the average number of frames can be correctly received by D within one time slot, and the higher the system throughput will be obtained. Moreover, although the throughput performance of protocols SOR-AP and SOR-V is similar under the same channel quality of link S-AP (AP-D) and link S-V (V-D), i.e., $p_1 = p_2 = 0.5$ and $q_1 = q_2 = 0.6$, the former is more recommended because choosing AP as the optimal relay can not only reduce the system complexity, but also be free of energy constraint, making it more effective than SOR-V protocol in the actual operation.

However, the above conclusions are inapplicable to energy efficiency shown in Figure 14 because there is no doubt that the more the relays involve in retransmissions, the higher the system energy will be consumed, especially the total transmitting energy consumption, making the relay cooperation shows superiority only under a communication scenario with larger d_{SD}. In particular, the channel quality in short distance communications ($d_{SD} < 380m$) is good, which makes the successful transmission probability of link

S-D very high. Instead of improving the system performance significantly, the introduction of relays increases the total energy consumption inevitably, making the advantage of energy efficiency between four protocols is shown as: Non-OR protocol > SOR-AP(V) protocols > DOR-APV protocol. However, the channel quality of link S-D decreases rapidly with the increase of d_{SD}, the outage probability of link S-D gets higher and the advantage of relay cooperation becomes more obviously, which is presented as with the increase of d_{SD}, the energy efficiency of protocols SOR-AP(V) and DOR-APV does not decline as fast as that of Non-OR protocol. Specifically, the SOR-AP(V) protocol achieves the best performance in medium distance communications ($380m < d_{SD} < 680m$) and DOR-APV protocol obtains the optimal energy efficiency in long distance communications ($680m < d_{SD} < 1000m$), which completely proves that with the increase of communication distance, (multiple) relay cooperation can indeed improve the system performance by providing more diversity gain with system, especially in terms of energy efficiency.

B. STUDY CASE 2: THE IMPACT OF THE LOCATION OF RELAYS ON SYSTEM PERFORMANCE

In order to evaluate the impact of the location of relays on system performance, the throughput and energy efficiency are depicted in Figure 15 and Figure 16 as a function of d_{SD} under different relay locations, respectively.

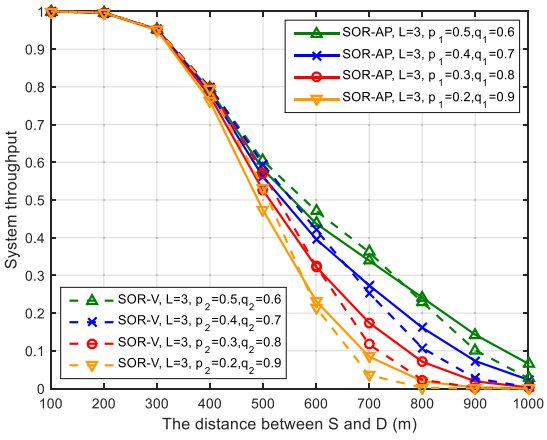

FIGURE 15. Study case 2: the impact of the location of relays on system throughput.

It can be seen firstly from Figure 15 and Figure 16 that both throughput and energy efficiency perform better as the location of relays gets closer to the middle position between S and D, i.e., $p_1, q_2 = 0.6, p_2, q_1 = 0.5$, which is because that the closer the location of relays gets to the middle of d_{SD}, the higher the SNR it can provide to the system, giving a theoretical reference for the design of future wireless cooperative network.

However, based on the conclusion drawn in study case 1 that SOR-AP protocol is more recommended than SOR-V protocol under the same channel quality of link S-AP (AP-D)

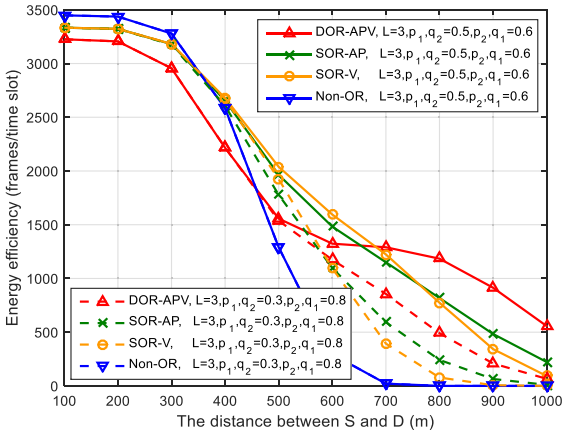

FIGURE 16. Study case 2: the impact of the location of relays on energy efficiency.

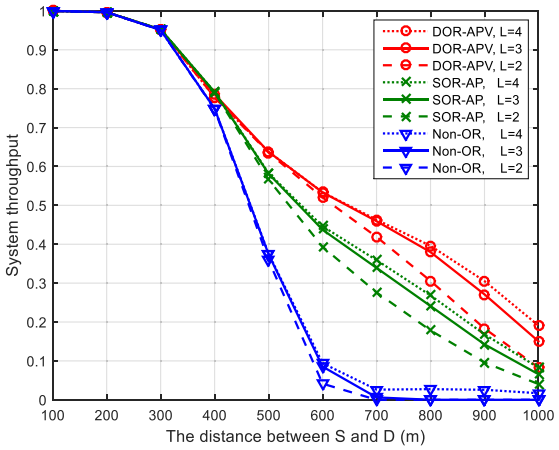

FIGURE 17. Study case 3: the impact of maximum transmission number on system throughput.

and link S-V (V-D), this case makes another important conclusion that SOR-V protocol is preferred over SOR-AP protocol in some situations due to the mobility of vehicles. In other words, D can decode the data frame more successfully transmitted from V than from AP when V gradually moves to the position closer to the middle of d_{SD} than AP, achieving a better performance improvement than SOR-AP protocol. Therefore, SOR-V protocol is more recommended when V has better channel quality than AP.

C. STUDY CASE 3: THE IMPACT OF MAXIMUM TRANSMISSION NUMBER ON SYSTEM PERFORMANCE

In order to evaluate the impact of maximum transmission number L on system performance, the throughput and energy efficiency are depicted in Figure 17 and Figure18 as a function of d_{SD} under different L, respectively.

It can be seen from Figure 17 and Figure 18 that both system throughput and energy efficiency are improved better under a larger L when $600m < d_{SD} < 1000m$, i.e., both of them are proportional to L, which is realistic because that the more the transmissions are performed, the more the payload

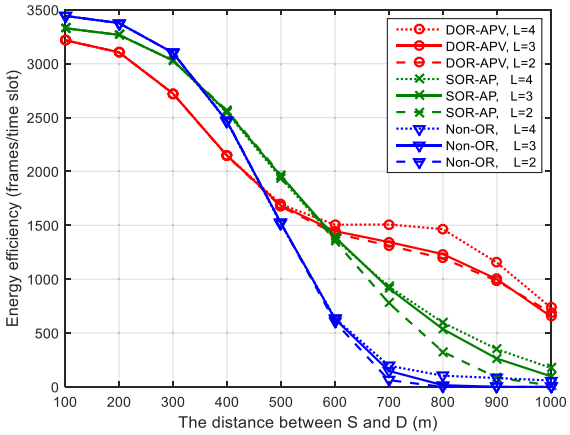

FIGURE 18. **Study case 3: the impact of maximum transmission number on energy efficiency.**

information can be transmitted in network, the lower the FER will be achieved and the more the average number of data frames will be transmitted correctly in one time slot, and thus the higher the throughput and energy efficiency will be achieved.

Another conclusion also can be drawn from Figure 17 and 18 that, as an important network parameter, the optimal value of L is not fixed, but closely related to the specific communication scenarios. For example, Because of the high SNR at D under the short distance communication ($d_{SD} < 380m$), the best value is $L = 2$. However, the optimal value of L gradually increases with the increase of communication distance (d_{SD}). In other words, more retransmissions are needed to compensate for the signal fading caused by the increase of communication distance. Therefore, Similar to the number of relays, the analysis and selection of optimal transmission number is another important research focus, which will be deeply studied in our future work.

To sum up, both system throughput and energy efficiency are proportional to the maximum transmission number, especially in medium and long distance communication scenarios.

VII. CONCLUSIONS

In this paper, four optimal relay selection protocols, which are named as Non-OR, SOR-AP, SOR-V and DOR-APV respectively, are firstly proposed for VANETs with HVC mode by introducing a four-node system model that considers communication links between relays, and then a generalized 2-dimensional DTMC model is established to obtain the closed-form expressions of system throughput and energy efficiency under arbitrary maximum transmission number for the four proposed protocols by analyzing their operational principle and outage probability. Finally, besides showing the effect of system parameters, such as the maximum transmission number and the location of relays, on system performance, the simulation results also make some conclusions by comparing the four proposed protocols, that is, on the SOR-AP(V) protocols side, SOR-AP protocol is more recommended than SOR-V protocol under the same channel quality of AP and V, but the latter is preferred when V has better channel quality than AP. Moreover, the four proposed protocols perform the best energy efficiency performance in short ($d_{SD} < 380m$), medium ($380m < d_{SD} < 680m$) and long ($680m < d_{SD} < 1000m$) distance communication scenarios, respectively, proving the close relationship between system performance and number of relays in wireless mobile communication networks.

In the future, our research will focus on the design of an adaptive wireless transmission mechanism (algorithm) that can dynamically coordinates the number of relays involved in retransmissions according to the changing communication distance, so as to achieve the optimal system performance.

REFERENCES

[1] B. Fiebig, "European traffic accidents and purposed solutions," in *Proc. ITU-T Workshop Standardisation Telecommun. Motor Vehicles*, May 2003, pp. 24–25.
[2] M. Jerbi, P. Marlier, and S. M. Senouci, "Experimental assessment of V2V and I2V communications," in *Proc. IEEE Int. Conf. Mobile Adhoc Sensor Syst.*, Oct. 2007, pp. 1–6.
[3] H. A. U. Mustafa, M. A. Imran, M. Z. Shakir, A. Imran, and R. Tafazolli, "Separation framework: An enabler for cooperative and D2D communication for future 5G networks," *IEEE Commun. Surveys Tuts.*, vol. 18, no. 1, pp. 419–445, 1st Quart., 2016.
[4] F. Wang, S. Li, Z. Dou, and S. Hai, "Performance analysis of a novel distributed C-ARQ scheme for IEEE 802.11 wireless networks," *KSII Trans. Internet Inf. Syst.*, vol. 13, no. 7, pp. 3447–3469, Jul. 2019.
[5] A. Chelli, J. R. Barry, and M. Pätzold, "Performance of hybrid-ARQ with incremental redundancy over double Rayleigh fading channels," in *Proc. IEEE 73rd Veh. Technol. Conf. (VTC Spring)*, May 2011, pp. 1–6.
[6] S. Li, Z. Dou, F. Wang, and Q. Xu, "Energy efficiency of five broadcast-based ARQ protocols in multi-hop wireless sensor networks," *IET Commun.*, vol. 13, no. 15, pp. 2243–2253, Sep. 2019.
[7] Y. Alghorani, G. Kaddoum, S. Muhaidat, S. Pierre, and N. Al-Dhahir, "On the performance of multihop-intervehicular communications systems over n*Rayleigh fading channels," *IEEE Wireless Commun. Lett.*, vol. 5, no. 2, pp. 116–119, Apr. 2016.
[8] S. Q. Nguyen and H. Y. Kong, "Outage probability analysis in dual-hop vehicular networks with the assistance of multiple access points and vehicle nodes," *Wireless Pers. Commun.*, vol. 87, no. 4, pp. 1175–1190, Aug. 2015.
[9] L. Xu, L. Huang, C. Cao, H. Wang, Y. Li, and T. A. Gulliver, "Outage performance of mobile V2V cooperative networks," *Phys. Commun.*, vol. 34, pp. 295–300, Jun. 2019.
[10] J. Zhang and G. Pan, "Secrecy outage analysis with Kth best relay selection in dual-hop inter-vehicle communication systems," *AEU-Int. J. Electron. Commun.*, vol. 71, pp. 139–144, Jan. 2017.
[11] T. T. Duy and H.-Y. Kong, "Performance analysis of incremental amplify-and-forward relaying protocols with Nth best partial relay selection under interference constraint," *Wireless Pers. Commun.*, vol. 71, no. 4, pp. 2741–2757, Aug. 2013.
[12] T. T. Duy, T. Q. Duong, D. B. da Costa, V. N. Q. Bao, and M. Elkashlan, "Proactive relay selection with joint impact of hardware impairment and co-channel interference," *IEEE Trans. Commun.*, vol. 63, no. 5, pp. 1594–1606, May 2015.
[13] H. Ilhan, "Performance analysis of cooperative vehicular systems with co-channel interference over cascaded Nakagami-m fading channels," *Wireless Pers. Commun.*, vol. 83, no. 1, pp. 203–214, Jul. 2015.
[14] T. Yang, X. Cheng, X. Shen, S. Chen, and L. Yang, "QoS-aware interference management for vehicular D2D relay networks," *J. Commun. Inf. Netw.*, vol. 2, no. 2, pp. 75–90, Jun. 2017.
[15] P. Belanovic, D. Valerio, A. Paier, T. Zemen, F. Ricciato, and C. F. Mecklenbrauker, "On wireless links for vehicle-to-infrastructure communications," *IEEE Trans. Veh. Technol.*, vol. 59, no. 1, pp. 269–282, Jan. 2010.
[16] D. Huakun, K. Xiaoyan, and X. Xuefeng, "RSU based communication capacity enhancement scheme for vehicular opportunistic networks," *Chin. High Technol. Lett.*, vol. 24, pp. 881–886, Sep. 2014.

[17] G. G. M. N. Ali, P. H. J. Chong, S. K. Samantha, and E. Chan, "Efficient data dissemination in cooperative multi-RSU vehicular ad hoc networks (VANETs)," *J. Syst. Softw.*, vol. 117, pp. 508–527, Jul. 2016.
[18] Z. Li, L. Jia, and F. Li, "Outage performance analysis in relay-assisted inter-vehicular communications over double-Rayleigh fading channels," in *Proc. IEEE Int. Conf. Commun. Mobile Comput.*, vol. 2, pp. 266–270, Apr. 2010.
[19] Z. Li, H. Hu, J. Li, and Y. Zhao, "Optimal power allocation method and outage probability analysis in AP-assisted inter-vehicular communications," in *Proc. 2nd Int. Conf. Comput. Automat. Eng. (ICCAE)*, vol. 5, Feb. 2010, pp. 102–106.
[20] J. Miller, "Vehicle-to-vehicle-to-infrastructure (V2V2I) intelligent transportation system architecture," in *Proc. IEEE Intell. Veh. Symp.*, Jul. 2008, pp. 715–720.
[21] M. Shirkhani, Z. Tirkan, and A. Taherpour, "Performance analysis and optimization of two-way cooperative communications in inter-vehicular networks," in *Proc. Int. Conf. Wireless Commun. Signal Process. (WCSP)*, Oct. 2012, pp. 1–6.
[22] S.-I. Sou, B.-J. Lin, and Y. Lee, "A probabilistic approach for V2V relay contention based on channel state information," in *Proc. IEEE Wireless Commun. Netw. Conf. (WCNC)*, Apr. 2013, pp. 505–509.
[23] S. H. Bouk, S. H. Ahmed, B. Omoniwa, and D. Kim, "Outage minimization using bivious relaying scheme in vehicular delay tolerant networks," *Wireless Pers. Commun.*, vol. 84, no. 4, pp. 2679–2692, May 2015.
[24] Q. Zheng, K. Zheng, P. Chatzimisios, H. Long, and F. Liu, "A novel link allocation method for vehicle-to-vehicle-based relaying networks," *Trans. Emerg. Telecommun. Technol.*, vol. 27, no. 1, pp. 64–73, Jan. 2016.
[25] F. Jameel, M. A. Javed, and D. T. Ngo, "Performance analysis of cooperative V2V and V2I communications under correlated fading," *IEEE Trans. Intell. Transp. Syst.*, early access, Jul. 30, 2019, doi: 10.1109/TITS.2019.2929825.
[26] H. Ghafoor and I. Koo, "Infrastructure-aided hybrid routing in CR-VANETs using a Bayesian model," *Wireless Netw.*, vol. 25, no. 4, pp. 1711–1729, May 2019.
[27] M. Usha and B. Ramakrishnan, "An enhanced MPR OLSR protocol for efficient node selection process in cognitive radio based VANET," *Wireless Pers. Commun.*, vol. 106, no. 2, pp. 763–787, Feb. 2019.
[28] X. Li, T. Song, Y. Zhang, G. Chen, and J. Hu, "Hybrid cooperative spectrum sensing scheme based on spatial-temporal correlation in cognitive radio enabled VANET," *IET Commun.*, vol. 13, no. 1, pp. 36–44, Jan. 2019.
[29] W. Wongtrairat and P. Supnithi, "Performance of digital modulation in double Nakagami-m fading channels with MRC diversity," *IEICE Trans. Commun.*, vol. E92-B, no. 2, pp. 559–566, 2009.
[30] A. G. Zaji, G. L. Stuber, T. G. Pratt, and S. Nguyen, "Statistical modelling and experimental verification for wideband MIMO mobile-to-mobile channels in urban environments," in *Proc. IEEE Int. Conf. Telecommun.*, Jun. 2008, pp. 1–6.
[31] M. Patzold, B. Hogstad, and N. Youssef, "Modeling, analysis, and simulation of MIMO mobile-to-mobile fading channels," *IEEE Trans. Wireless Commun.*, vol. 7, no. 2, pp. 510–520, Mar. 2008.
[32] A. Chelli and M. Patzold, "The impact of fixed and moving scatterers on the statistics of MIMO vehicle-to-vehicle channels," in *Proc. VTC Spring - IEEE 69th Veh. Technol. Conf.*, Apr. 2009, pp. 1–6.
[33] H. Zhiyi, C. Wei, Z. Wei, M. Patzold, and A. Chelli, "Modelling of MIMO vehicle-to-vehicle fading channels in T-junction scattering environments," in *Proc. 3rd Eur. Conf. Antennas Propag.*, Mar. 2009, pp. 652–656.
[34] V. I. Kostylev, "Distribution of the sums of squares of moduluses of complex-joint Gaussian random values with the correlation matrix of a simple structure," *Radioelectron. Commun. Syst.*, vol. 44, no. 5, pp. 37–40, Feb. 2001.
[35] H. Chen, Y. Cai, W. Yang, D. Zhang, and Y. Hu, "Throughput and energy efficiency of a novel cooperative ARQ strategy for wireless sensor networks," *Comput. Commun.*, vol. 35, no. 9, pp. 1064–1073, May 2012.
[36] I. S. Gradshteyn and I. M. Ryzhik, "Table of integrals, series and products," *Math. Comput.*, vol. 20, no. 96, pp. 1157–1160, Jan. 2007.

SUOPING LI (Member, IEEE) received the B.Sc. degree in mathematics from Northwest Normal University, in 1986, the M.Sc. degree in stochastic model with applications from Lanzhou University, in 1996, and the Ph.D. degree in signal and information processing from Beijing Jiaotong University, China, in 2004. He was a Visiting Scholar with the Swiss Federal Institute of Technology Zurich (ETH), from May 2007 to May 2008, and also a Visiting Professor with American East Texas Baptist University (ETBU), from August 2011 to December 2011. He completed short academic visits at the Universite de Technologie Belfort-Montbeliard (UTBM), France, in 2017, and the Università degli Studi dell'Aquila (UNIVAQ), Italy, in 2018. He is currently a Full Professor with the School of Science, Lanzhou University of Technology (LUT), China. His primary research interests include stochastic control theory and applied stochastic process, stochastic modeling analysis of wireless communication systems, cooperative communications, ad hoc networks, cognitive radio networks, and wireless sensor networks.

FAN WANG received the B.S. degree in telecommunication engineering from the Tianjin University of Commerce, China, in 2014. She is currently pursuing the Ph.D. degree in control theory and control engineering with the Lanzhou University of Technology, China. Her research interests include stochastic modeling analysis of wireless communication systems and wireless sensor networks.

JAAFAR GABER (Member, IEEE) received the Ph.D. degree in computer science from the University of Science and Technology of Lille, Lille, France, in 1998. He was a Research Scientist with the Institute of Computational Sciences and Informatics, George Mason University, Fairfax, VA. He is currently an Associate Professor of computational sciences and computer engineering with the University of Technology of Belfort-Montbeliard, France. His research interests include high-performance computing, parallel processing and distributed systems, and experimental performance evaluations.

XIAOKAI CHANG received the M.Sc. degree in applied mathematics from Liaoning Technical University, China, in 2011, and the Ph.D. degree in applied mathematics from Xidian University, China, in 2019. He is currently a Lecturer with the School of Science, Lanzhou University of Technology (LUT). His research interests include numerical algorithm, nonlinear optimization, and operator splitting.